CHALMERS
UNIVERSITY OF TECHNOLOGY

UNIVERSITY OF GOTHENBURG

Stepped Frequency Modulated Continuous Wave in Guided Wave Radar

Master's thesis in Embedded Electronic System Design

EMIL ZACHARIA GEORGE

Department of Computer Science and Engineering
CHALMERS UNIVERSITY OF TECHNOLOGY
UNIVERSITY OF GOTHENBURG
Gothenburg, Sweden 2024

Master's thesis 2024

Stepped Frequency Modulated Continuous Wave in Guided Wave Radar

EMIL ZACHARIA GEORGE

UNIVERSITY OF
GOTHENBURG

CHALMERS
UNIVERSITY OF TECHNOLOGY

Department of Computer Science and Engineering
Chalmers University of Technology
University of Gothenburg
Gothenburg, Sweden 2024

Stepped Frequency Modulated
Continuous Wave in Guided Wave Radar
EMIL ZACHARIA GEORGE

Supervisor: Lars Svensson, Department of Computer Science and Engineering
Company advisor: Prabhat Khanal, Emerson Rosemount Tank Radar AB
Examiner: Per Larsson-Edefors, Department of Computer Science and Engineering

Master's Thesis 2024
Department of Computer Science and Engineering
Chalmers University of Technology and University of Gothenburg
SE-412 96 Gothenburg
Telephone +46 31 772 1000

Typeset in LaTeX
Gothenburg, Sweden 2024

Stepped Frequency Modulated
Continuous Wave in Guided Wave Radar
EMIL ZACHARIA GEORGE
Department of Computer Science and Engineering
Chalmers University of Technology and University of Gothenburg

Abstract

In industries, level measurement has to be precise and fool-proof at a minimal cost and power consumption. Radar technologies are used in this field along with other float, pressure, and magnetic based instruments. Guided wave radars (GWR) are used to measure levels and multiple material interfaces in a tank containing bulk liquids, solids, or slurries. The existing GWR device sends a short DC pulse down the waveguide made of a stiff metallic rod, flexible wire, or a coaxial construction which hits the media and a small proportion of the energy is reflected back to the device. The level is directly proportional to the time elapsed between the transmission of the pulse from the radar and the reception of the echo from the target.

The use of frequency-modulated continuous waves (FMCW) is expected to improve the accuracy and reliability of the level measurements. Existing non contacting radars (NCR) transmit a frequency modulated signal chirp within a fixed bandwidth through an antenna. A part of this transmitted signal is reflected back by the material whose level is being measured inside the tank. This reflected signal is received back at the radar. The level of the contents of the tank is established by comparing the frequencies of the transmitted and received signals. An initial study on generating a low-frequency FMCW signal, sending it over a waveguide, and receiving it was done internally at Emerson using a Vector network analyzer (VNA) and found that an FMCW based GWR is feasible.

A wider bandwidth in the range of multiple gigahertz (GHz) is required in FMCW to improve the resolution of the targets and a frequency sweep starting from DC or very low frequencies is preferred to get the signed values of the targets and echoes in the echo curve. A traditional FMCW radar requires phase linearity in their transmitted signal. Maintaining phase linearity for the transmitted signal from near DC to multiple GHz is not possible. Therefore, a FMCW technology achieved by stepping in frequency is proposed in this thesis where the phase linearity of the transmitted signal is not necessary. This introduces two main constraints in the Stepped-FMCW GWR, namely the power consumption and measuring time. The objective of this thesis work was to setup and demonstrate a Stepped-FMCW GWR concept operating over DC to 4 GHz range and study its power consumption and measurement time.

The demonstration setup consist of two frequency synthesizers together covering the frequency range from 1 MHz to 4 GHz, radio frequency (RF) gain blocks, mixers, switches, variable attenuator, variable potentiometer, intermediate frequency (IF) filter, IF amplifier and a microcontroller (MCU). The measurement is done by generating a 10 kHz offset sweep for the entire frequency range along with the transmitted

sweep and sampling this offset IF signal for amplitude and phase response. The MCU controls the frequency synthesizers and other variable components via its serial and parallel input/ output (IO) interfaces, and samples the IF signal using its analog to digital converter (ADC) channel. The compatible digital signal processor (DSP) library functions are used for filtering and performing inverse fourier transform to generate the echo curve showing the targets.

The process proved the feasibility of developing a printed circuit based system for the stepped FMCW GWR. The results showed that the demonstrator is capable of measuring level at a good accuracy in a reasonable time. The power measurements were higher for the system. But, as the demonstrator is designed using evaluation kits, the power measured include additional power consumption of those components not used. Design of a dedicated custom board in future is expected to provide more accurate power measurements. Also, adding power control options for the RF gain blocks and mixers could optimize it further. Regarding the measurement time, there is room for further improvements by the choice of frequency range and the frequency synthesizer components.

Keywords: bandwidth, GWR, level measurement, phase linearity, stepped FMCW.

Acknowledgements

I would like to give my sincerest thanks to my supervisor Lars Svensson and advisor Prabhat Khanal who have given much needed guidance during this thesis. Also, I express my thanks to all the other different people of Emerson Rosemount Tank Radar AB who answered my questions and supported me. I would also like to thank the examiner Per Larsson-Edefors for all his insightful feedback and support. I would like to dedicate this thesis to my dearest Amma Reena and Appa George who insisted me on continuing with the thesis during the most challenging times.

Emil Zacharia George, Gothenburg, September 2024

List of Acronyms

Below is the list of acronyms that have been used throughout this thesis listed in alphabetical order:

GWR	Guided Wave Radar
NCR	Non Contacting Radar
FMCW	Frequency Modulated Continuous Wave
RF	Radio Frequency
IF	Intermediate Frequency
MCU	Microcontroller Unit
ADC	Analog to Digital Converter
VCO	Voltage Controlled Oscillator
DSP	Digital Signal Processing
IDFT	Inverse Discrete Fourier Transform
IFFT	Inverse Fast Fourier Transform
SPDT	Single Pole Double Throw
I2C	Inter Integrated Circuit
SPI	Serial Peripheral Interface
UART	Universal Asynchronous Receive Transmit
PCB	Printed Circuit Board
HF	High Frequency
LF	Low Frequency
LO	Local Oscillator
GPIO	General Purpose Input Output
SNR	Signal to Noise Ratio

Contents

1

Introduction

Level measurement, which is essential across various industries, involves gauging the quantity of liquid or solid within a container. Its applications span across industrial process control, water treatment, storage tank management, etc. It involves the detection of substances, measurement of accurate levels, and the monitoring of real-time changes. This is integral to ensuring operational safety and efficiency in almost all industrial processes [1].

The different parameters used for level measurement include capacitance, hydrostatics, magnetics, ultrasonics, microwaves, mechanical floaters, etc. In capacitive level measurement, the sensor and the vessel form the two electrodes of a capacitor. Any change in level causes a capacitance change, which in turn is converted into a level signal. But, capacitive liquid level gauges have high dependence on the dielectric constant of the liquid. A hydrostatic level sensor is a form of level probe that is used especially for level monitoring, by measuring the hydrostatic pressure in a virtually static liquid, at a pre-determined level of submersion. Its major limitation is that it only works on liquids. Magnetic level indicators consist of a chamber, a magnet equipped float which rises and lowers with the fluid level, and an indicator which is mounted on the chamber. They provide robust, low maintenance measurements in oil, gas, petrochemicals, and in power applications. But they cannot be used in severely turbulent, dirty, foaming, fouling services or in cases where there is presence of solid particles, like sand in the fluid.

In non-contact ultrasonic level measurement, the sensor emits ultrasonic pulses in the direction of the medium, a part of which is reflected back. The elapsed time from emission to reception of the signals is proportional to the level in the tank. Ultrasonic sensors are ideal for simple standard applications, both for liquids and solids. But using an ultrasonic level sensor for solids' level measurement usually reduces the effective range of the sensor by half [2]. Also, tanks with dust or powders, scatter sound waves leading to erroneous readings.

Radar level transmitters generate and direct the microwave signals downwards into a tank. When they reach the interface between the low dielectric and the higher dielectric liquid or solid, some part of the transmitted signals are reflected back to the level transmitter. The level is estimated by measuring the time elapsed between the transmitted and received signals. Radar based level measurement instruments can be broadly classified based on the mode of propagation of the microwaves - Guided Wave Radars (GWR) and Non-Contacting Radars (NCR). GWRs use transmission lines made of a stiff metallic rod or flexible wire or a coaxial construction. They

are capable of measuring continuous level and interface level of liquids, solids, and slurries. NCRs use an antenna to guide the signals inside the tank and do not come in direct contact with the medium being measured. They also measure continuous level of liquids or solids in small and large tanks, vessels and open-air applications across many different industries [3]. Radar level transmitters when compared to ultrasonic level sensors are less affected by temperature and pressure, improving consistency and accuracy. Radar level sensors are also well suited for speciality applications, such as working in a vacuum or in high pressures. Radars are also less affected by foam, vapours, powders, and dust which may interfere with signals on ultrasonic level sensors and lead to erroneous readings. A simplified diagram for a GWR is shown in figure 1.1.

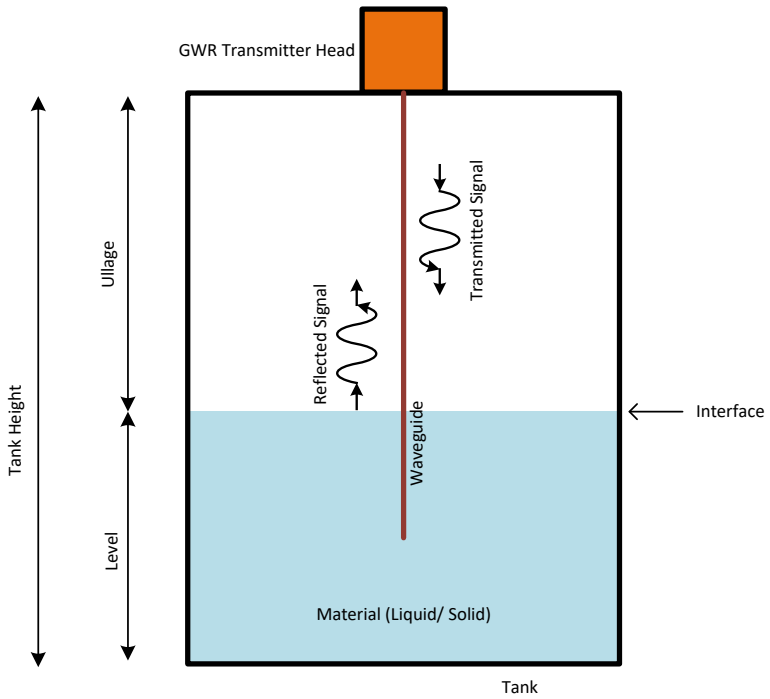

Figure 1.1: Simplified working diagram of GWR

1.1 Related Work

The use of stepped frequency modulated continuous wave (FMCW) in GWR level measurement applications is not common. The stepped frequency signal generation and reception over the air for detection in biomedical applications was part of a master thesis done few years ago [4]. They designed a system using off-the-shelf components and were able to see a good agreement between measured and simulated results for distances up to 2 meters. The use of stepped FMCW in synthetic aperture radar has already been studied [5]. The simulation study on the use of stepped frequency continuous waves (SFCW) in ground penetrating radar (GPR) for detecting objects buried beneath the earth's surface or hidden behind the wall [6] could measure the range of an object upto 2 m distance. They use 1.5 GHz band-

width over 2 GHz carrier in the simulation. The received signals which consist of complex signals are passed through an inphase/ quadrature demodulator (I/Q demodulator) into inphase and quadrature signals. These are filtered, digitized using ADC, and inverse fast fourier transform (IFFT) is applied for the phase difference in inphase and quadrature signals of the reflected signal. This is possible assuming clean signals in each frequency step. The FMCW GWR design is inspired by the low-cost network analyzer design found in [7]. It has a frequency synthesizer circuit which can switch between two ports while transmitting. On the receiving side, apart from the one receiver which can be switched between both the ports, there was another one to get the transmitted reference for calibration. The use of separate devices for low frequencies upto 50 MHz, which was a direct digital synthesis (DDS) integrated circuit (IC), and a fractional-N phase locked loop (PLL) with voltage controlled oscillator (VCO) for the higher frequencies motivated us on the mode of sweep generation. The source selection in the circuit was through RF switches. The gain block was introduced as the measured transmitted power and the reflected power was very small for the higher range of low frequency synthesizer.

1.2 Purpose and Goal

This thesis aims to study, develop, and experiment if the stepped FMCW technology can be employed in GWR devices to replace the traditional pulsed technology. The comparison will be in cost, power consumption, and measurement time.

The goal of this project is to demonstrate a stepped FMCW GWR with off-the-shelf microwave and control component development kits which can generate a sweep of microwave frequencies from 1 MHz to 4 GHz with 1 MHz step. The radar should send it over a rigid metallic transmission line, receive the reflected signal from a target and process the received signal to detect the target's range. The radio frequency (RF) signals shall be generated using two PLL based VCO controlled by a microcontroller unit (MCU). The reflected RF signal is to be converted to an intermediate frequency (IF) signal and sampled using an inbuit ADC which is part of the MCU. The sampled signals of the entire sweep which are in frequency domain should be converted to a time domain signal by applying IFFT inside the digital signal processing (DSP) blocks of the same MCU. The echo curve obtained has to be evaluated, optimized; and final measurements in real tanks are to be performed.

1.3 Thesis Outline

This report provides detailed information on the topic. Chapter 2 provides the theoretical foundations of microwave hardware design for frequency sweep generation, reception, and control. It also provides information on the MCU control circuits, interfaces, and the related software algorithms. The theoretical calculations on the basis of FMCW and stepped FMCW based level measurement are included in this same chapter. The basic signal processing steps involved like the filtering, IFFT are also explained in detail. Chapter 3 explains the research approach, tools used in the thesis project, scope limitations, and assumptions. Chapter 4 consists of the design

of the system hardware, software and signal processing used. Chapter 5 presents the results obtained from the different tests performed with the designed radar circuit. Chapter 6 discusses further on the results presented in the previous chapter. Chapter 7 summarizes the major findings like advantages, limitations, future of the scope of the research, and final reflections on the thesis project.

2

Theoretical Background

This chapter provides a theoretical information on all the hardware and software modules used in the stepped FMCW radar demonstration setup. A good understanding of the area of GWR is very helpful to design and develop a stepped FMCW GWR prototype and study its parameters. The content of the tank, tube or the container is considered as the target to which the distance is measured. This section provides a general overview of the existing technology used in GWR, the microwave and control circuits involved in a GWR system and the signal processing techniques associated with the FMCW and stepped FMCW technology.

2.1 Existing Radar Technologies

The two types of radar in use for level measurement are pulsed radar and FMCW radar. Pulsed technology is mostly used in GWRs whereas FMCW is in NCRs.

2.1.1 Pulsed Radar

The current technology used in GWR is pulsed signaling. The device emits a low-energy microwave pulse along a probe, which on encountering the target, reflects some of its energy back to the device. The level measurement directly correlates with time delay between transmitted pulse and the received echo from the target. As a portion of the emitted pulse persists down the probe, it can also measure levels of different materials in the same tank,and their interfaces. An example would be a tank containing multiple materials like air, oil and water. The transmitted and received pulse signals are sampled in the time domain. The time duration between the transmission and reception of the pulse is used to calculate the distance to the target making use of the speed of an electromagnetic wave as shown in figure 2.1.

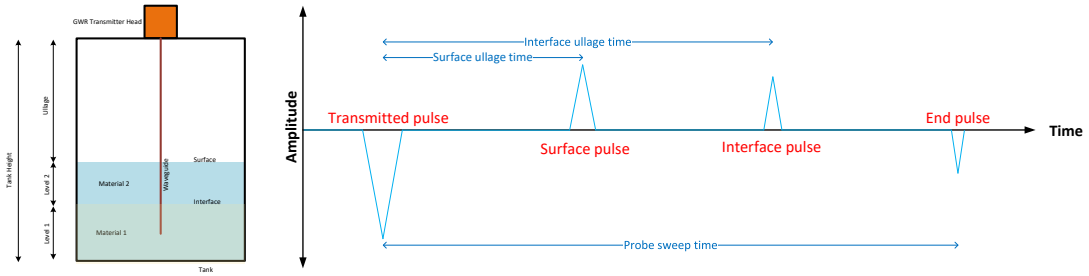

Figure 2.1: Pulsed Signaling in GWR

The range of the radar can be expressed as below.

$$R = \frac{c \cdot \Delta t}{2\sqrt{\epsilon_r}} \tag{2.1}$$

Here, R is the distance to target, c is the speed of electromagnetic wave in free space, Δt is the time difference between transmitted and received pulse and ϵ_r is the dielectric constant of the medium. The received pulse can be a surface pulse, an interface pulse or an end pulse. The pulsed technology has several constraints like it needs a high-power transmitter to generate the pulse as the energy exists only for a short pulse and needs to travel across multiple interfaces. Narrower the pulse, higher is the resolution. However, being narrow also decreases the total transmitted energy, which in turn decrease radar sensitivity. Therefore the radar bandwidth and transmitted power are dependent. Due to the limit on the maximum allowed pulse amplitude, one cannot increase power to compensate for the decrease in energy within the narrower pulse. Also, as the pulsed radar works in time domain, the effect of noise and false triggering which comes up as part of the electromagnetic interference (EMI) issues also needs to be dealt with.

2.1.2 FMCW Radar

FMCW radar is a continuous power transmitting radar that changes its operating frequency continuously within a defined bandwidth during the level measurement [8]. A signal which increases or decreases in frequency periodically is transmitted to the target. When the target reflects an echo signal and this echo is received back at the radar, that change of frequency gets a delay in time as shown in figure 2.2. As the echo cannot be measured directly in time like the pulse technique, the differences in phase or frequency between the transmitted and the received signal is measured and analyzed to derive the distance.

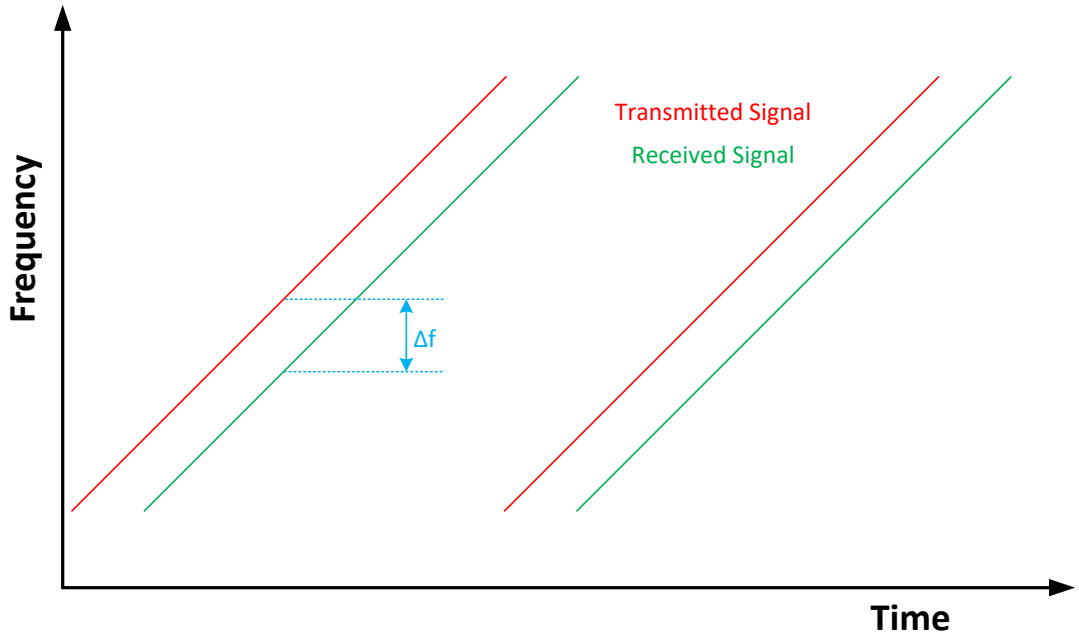

Figure 2.2: FMCW Signaling in NCR

It needs to maintain a linear phase along the frequency sweep throughout the bandwidth. FMCW radars have comparatively smaller bandwidth as maintaining phase linearity over larger bandwidth like multiple GHz frequencies is not easy.

2.2 Stepped FMCW Radar

An FMCW radar with increased accuracy, sensitivity, stability, and EMC performance is assumed to possess the potential to replace the pulse technology that is used in Emerson 3300 [9] and 5300 [10] GWR gauges today.

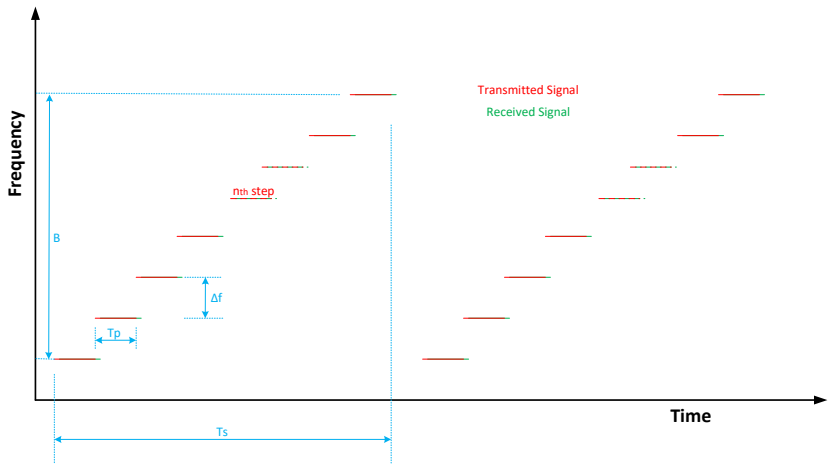

Figure 2.3: Stepped FMCW Signaling

As shown in figure 2.3, the radar waveform consists of a series of sinusoidal waves

with frequency increasing linearly. Here, Δf is the frequency step size, N is the number of steps, B is the bandwidth of the radar, Δt is the time step size and T_s is the time of a measurement sweep. The radar measures the phase and amplitude of each frequency and uses the Inverse Fourier Transform (IFT) to generate a time domain signal. An echo curve is a graph with amplitude plotted against distance showing each reflected echo received by the radar along the transmitted signal's path. A wider bandwidth is preferred to improve the resolution of the targets.

A detailed understanding on the different microwave circuits, digital control circuits, communication interfaces, signal processing techniques, are all helpful for the reader to understand the further design and methods used.

2.3 Frequency Synthesizers

Frequency synthesizers are electronic devices that are capable of generating a set frequency from a combination of other frequencies. They are commonly used in communication devices including mobile phones, navigation systems, and in radars. The mode of generation divides them into direct analog synthesis (DAS) and direct digital synthesis (DDS). In DDS, digital circuits generate a time-varying signal in digital form and a digital to analog converter (DAC) converts it to a continuous analog signal. In DAS, a reference oscillator is used for the reference frequency along with a VCO and PLL. They may also use a range of prescalers and frequency dividers to extend their frequency range and increase bandwidth. DDS has higher performance over a wider range of frequencies with fine resolution, but also is more expensive. In contrast, PLL based DAS is capable of RF signal generation at a lower expense. As FMCW technology does not require a very accurate frequency source, a PLL based DAS is enough.

Phase Locked Loop (PLL)

PLL is a closed loop feedback system that includes a VCO, phase detector, and low pass filter within its loop. It generates an output signal whose phase is fixed relative to the phase of an input signal, thereby providing stable output frequency. The internal diagram of a PLL is shown in figure 2.4.

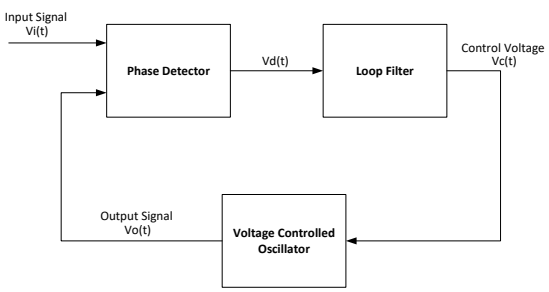

Figure 2.4: Block Diagram of a PLL

Voltage Controlled Oscillator (VCO)

VCO is an electronic oscillator circuit whose frequency can be controlled using a DC input voltage. The oscillation is normally produced by transferring energy between different forms like electric and magnetic field. Commonly, VCO has an inductor (L) and a capacitor (C) transferring energy between them. The oscillation frequency is the resonant frequency inversely proportional to $\sqrt{LC}$. Voltage Controlled Crystal Oscillator (VCXO) is an oscillator whose output frequency varies based on the applied control voltage. A VCXO is made up of a crystal, an oscillator circuit, a varactor diode and associated circuits. It has higher stability and lower phase noise, but supports only a lower frequency range compared to VCO.

2.4 Other Microwave Components

Along with the frequency synthesizer, the microwave circuit includes mixer, amplifier, attenuator, resistive bridge, etc.

Directional Coupler As the transmitted and the received signals travel through the same connection point to the transmission line, the incoming waves and the outgoing waves are to be separated. The directional coupler is a passive device that separates the forward and backward waves in a transmission line. The working of a directional coupler in a radar is shown in figure 2.5.

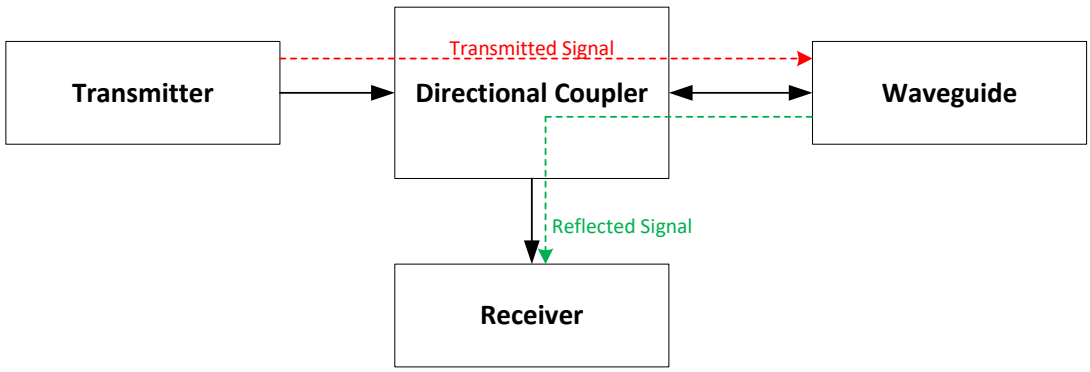

Figure 2.5: Working of directional coupler

Loaded Resistive Bridge Resistive couplers normally operate in a very wide bandwidth of frequencies. The bridge circuit in figure 2.6 is similar to a Wheatstone's bridge, but it is not expected to be balanced. Here, R_L depicts the transmission line leg, V_{TX} is the transmitted signal, and V_{RX} measured across $R4$ is the reflected signal. As the microwave trace impedance is 50 Ω, the bridge should be matched with no output across V_{RX}, when R_L is terminated by 50 Ω to the ground. As the ratio between $R1$ and $R2$ should be matched to $R3$ and R_L, $R1$= 50 Ω, $R2$= 50 Ω, and $R3$= 5.55 Ω. $R4$ and R_s are also chosen to be 50 Ω for impedance matching.

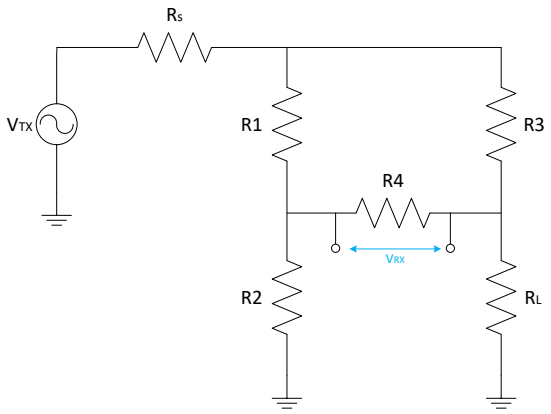

Figure 2.6: Resistive bridge circuit acting as directional coupler

RF Attenuator An RF attenuator helps in controlling the amplitude of the RF signals. They normally contain a series of resistors chosen to match the 50 Ω characteristic impedance of the transmission line. They are arranged in a T or π configuration where the input impedance and output impedance match the impedance of the system. This helps in minimizing the signal reflection and loss.

RF Gain Block An RF gain block is a broadband amplifier with a fixed gain for a wide range of frequencies. It has a low noise figure, higher linearity and is internally matched to 50 Ω at the input and output.

RF Switch RF switches are used to control the path of the RF signals in a circuit. They have very low insertion loss for a wide frequency band. A single pole double throw (SPDT) switch has a common port and two channel ports as shown in figure 2.7. The control signals can be used to route a signal in the common port to one among the two channel ports or vice versa.

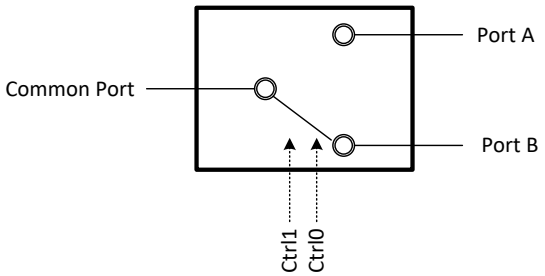

Figure 2.7: SPDT RF Switch

RF Mixer An RF mixer is a three-port passive or active device that can change the frequency of an electromagnetic signal while preserving the phase and amplitude of the initial signal. It has two input ports and an output port as shown in figure 2.8. The sum and difference of the input signal frequencies are available at the output.

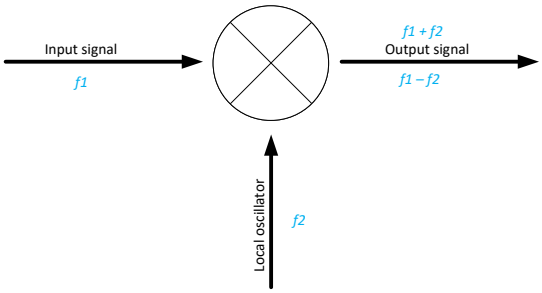

Figure 2.8: RF mixer

RF Switch As Mixer An SPDT RF switch can function as an RF mixer when the RF input is given at one of its inputs and a ground on the other. The switching between these two channels is done based on the CMOS control inputs. When the IF frequency signal is connected across these control inputs, the common port gets the ground and the RF signal alternatively based on the IF frequency. In effect, the switch multiplies the RF frequency by the IF frequency.

Balun Transformer A balun is a type of transmission line transformer. It is a two-port component that is placed between a source and load when a differential symmetric RF functional block needs to be connected to a single-ended block. The differential signals will be connected to one side of the transformer whereas one terminal on the other side will be grounded as shown in figure 2.9.

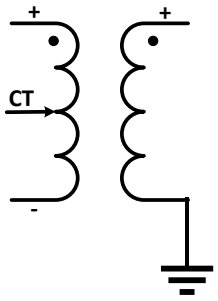

Figure 2.9: Balun transformer

2.5 Control Circuit

The control circuit consists of the microcontroller for the complete system control, signal processing and communication. It also include the IF filter and amplifier circuit designed to obtain a stable IF signal to sample at the ADC. A digital potentiometer helps in controlling the analog amplifier circuit from an MCU.

Microcontroller (MCU) The modern MCU can function as a controller, digital signal processor (DSP), Analog to digital converter (ADC), etc. The STM32U575 controller is based on Arm Cortex-M33 processor core running at 160 MHz. It has

digital signal processing and a floating-point unit (FPU) for the signal processing actions. It also offers 2 Mb flash memory storage. The options for peripheral interface include serial peripheral interface (SPI), inter integrated circuit (I2C), universal asynchronous receive transmit (UART), etc. There are a large number of general purpose input output (GPIO) pins also for parallel control. The two ADC channels are of 14-bit and 12-bit resolution capable of 2.5 Msps sampling rate.

IF Filter And Amplifier An IF filter circuit attenuates the signals above its cutoff frequency. The amplifier circuit helps to maintain the amplitude of an IF signal which can be sampled by the ADC of the MCU. It can also convert the differential outputs to a single-ended signal which can be interfaced to the analog input of an MCU. They are designed using operational amplifier (opamp) circuits.

Digital Potentiometer Potentiometer is a variable resistor with two end probes and a wiper. The resistance across the end probes is finite where the position of the wiper changes the resistance between each of the end probes to the wiper. A digital potentiometer is a similar resistor ladder network which can be controlled by digital control inputs.

2.6 FMCW Level Measurement Principle

Assume an FMCW sweep with bandwidth (B Hz), and the sweep takes T_s seconds to complete. Then the frequency change rate is B/T_s Hz/s. For a target placed at a distance of h meters, the travel time for the microwave signal is $2h/c$ seconds, where c is the speed of an electromagnetic wave. As the frequency changes at a rate of B/T_s Hz/s, the difference in frequency between the transmitted and received signal will be Δf Hz.

If the target is in motion along the sweep, Doppler coupling comes prevalent. Doppler effect is the change in frequency due to the relative motion of the source and the receiver. The Doppler shift equation is defined as

$$\Delta f = f_r - f_t \tag{2.2}$$

where Δf represents the Doppler shift, f_r is the reflected frequency, and f_t is the transmitted frequency. Considering v as the velocity of the target,

$$f_r = \frac{2h}{c} \cdot \frac{B}{T_s} + \frac{2vf_t}{c} \tag{2.3}$$

For normal velocities in level measurement applications, the Doppler shift has a very minor influence on the measured distance. The FMCW signal flow is shown in figure 2.10.

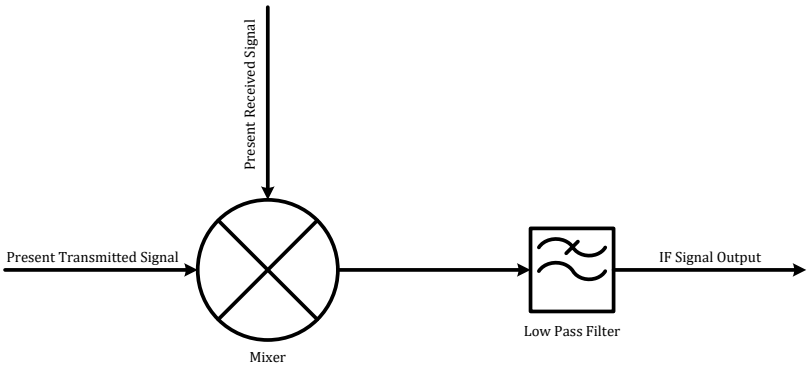

Figure 2.10: FMCW signal flow

Consider the FMCW signal sweep shown in figure 2.11. The frequency of a linear FMCW radar transmitted signal can be expressed as

$$\omega(t) = \omega_0 + \Delta\omega \cdot \frac{t}{T_s} \tag{2.4}$$

The phase of a linear FMCW radar transmitted signal can be expressed as

$$\Phi(t) = \int \omega(t)\, dt = \int \omega_0 + \Delta\omega \cdot \frac{t}{T_s}\, dt = \omega_0 t + \frac{\Delta\omega \cdot t^2}{2T_s} \tag{2.5}$$

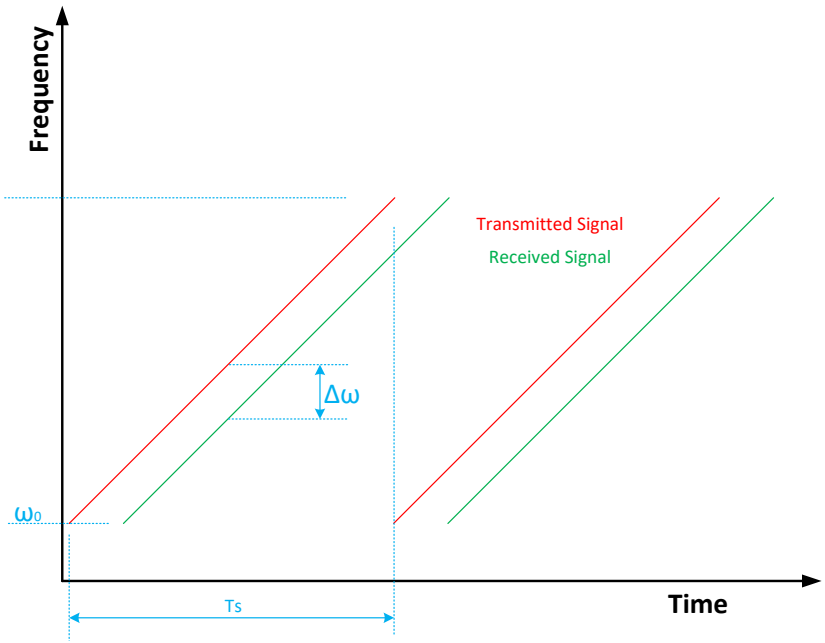

Figure 2.11: FMCW signal sweep with start frequency (ω_0) and frequency step ($\Delta\omega$)

The phase of the received signal from a single echo can thereby be expressed as

$$\Phi(t-\tau) = \omega_0(t-\tau) + \frac{\Delta\omega \cdot (t-\tau)^2}{2T_s} \tag{2.6}$$

where $\tau = \frac{2h}{c}$ is the travel time for the microwave signal.

The transmitted signal is mixed with the received signal to get an IF signal which after low-pass filtering gives a phase in equation 2.7.

$$\Phi_{IF}(t) = \omega_0 \tau + \frac{\Delta\omega\tau t}{T_s} - \frac{\Delta\omega\tau^2}{T_s} \tag{2.7}$$

The frequency of the signal is expressed in equation 2.8

$$\omega_{IF} = \frac{\partial\Phi}{\partial t} = \frac{\Delta\omega}{T_s} \cdot \tau \tag{2.8}$$

The IF signal contains a number of sine components whose frequency and phase are directly proportional to the distance to the targets, where the transmitted signals were reflected. The amplitude of the same IF signal will be proportional to the reflection coefficient of the targets. The distance to target h is calculated as

$$h = \frac{T_s \cdot \omega_{IF} \cdot c}{2\Delta\omega} \tag{2.9}$$

$$h = \frac{\Phi_{IF}(0) \cdot c}{2 \cdot \omega_0} \tag{2.10}$$

Note than we have ignored the term with τ^2 while deriving above equation.

2.7 Stepped FMCW Level Measurement Principle

The stepped FMCW radar uses a sequence of single-frequency pulses, and the frequency of each pulse is increased in uniform steps as shown in figure 2.12.

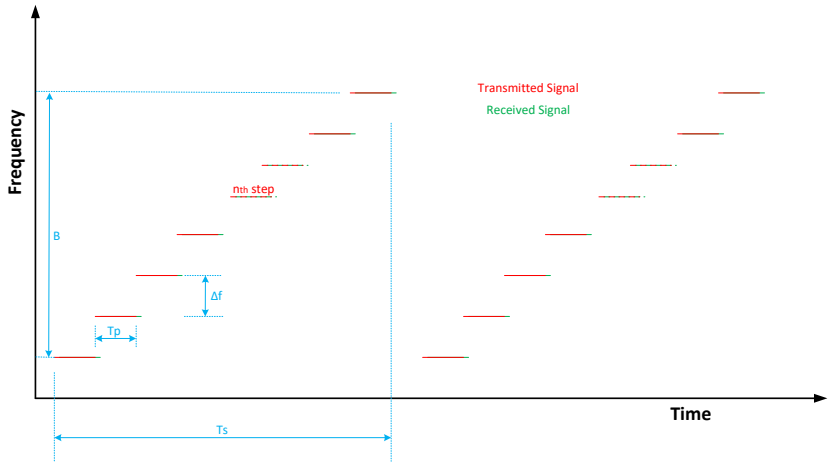

Figure 2.12: Stepped FMCW Signal Sweep

The stepped frequency waveform can be considered as the frequency sampling points of the total bandwidth. Here, the radar only needs to process a single-frequency

signal at a time [5]. The stepped frequency waveform uses a sequence of pulses to achieve ultrawide bandwidth, where each pulse has a single frequency. This sequence of pulses can be considered as the frequency sampling of the total bandwidth in the frequency domain. The transmitted waveform can be represented as equation 2.11.

$$S_t(n,t) = \text{rect}\left(\frac{t}{T_p}\right) \cdot \exp\left(j2\pi f(n)t\right) \tag{2.11}$$

where n is the frequency step number ranging from 1 to N where N is the total number of steps in the sweep. T_p is the time for one frequency pulse and $f(n)$ is the frequency of the nth step.

For a target at a distance h, the reflected signal can be expressed as

$$S_r(n,t) = \text{rect}\left(\frac{t-\frac{2h}{c}}{T_p}\right) \cdot \exp\left(j2\pi f(n)\left(t-\frac{2h}{c}\right)\right) \tag{2.12}$$

where c is the speed of the microwave signal. Here the reflection coefficient of the target is not taken into consideration.

A local oscillator signal with the frequency for the particular step will be used as the reference signal to demodulate the received signal.

$$S_{\text{LO}}(n,t) = \exp(j2\pi f(n)t) \tag{2.13}$$

The demodulated IF signal can be expressed as

$$S_{\text{IF}}(n,t) = S_r(n,t) \cdot S^*_{\text{LO}}(n,t) \tag{2.14}$$

$$S_{\text{IF}}(n,t) = \text{rect}\left(\frac{t-\frac{2h}{c}}{T_p}\right) \cdot \exp\left(-j\frac{4\pi f(n)h}{c}\right) \cdot \exp(-j2\pi f(n)t) \tag{2.15}$$

$$S_{\text{IF}}(n,t) = \text{rect}\left(\frac{t-\frac{2h}{c}}{T_p}\right) \cdot \exp\left(-j\left(\frac{4\pi f(n)h}{c}\right)\right) \tag{2.16}$$

Assuming f_0 as the starting frequency of the sweep. It means $f(1) = f_0$. If the frequency step is denoted as Δf, the frequency of nth step can be expressed as $f(n) = f_0 + n\Delta f$. Applying this to equation 2.16 gives

$$S_{\text{IF}}(n,t) = \text{rect}\left(\frac{t-\frac{2h}{c}}{T_p}\right) \cdot \exp\left(-j\frac{4\pi f_0 h}{c} - j\frac{4\pi\Delta f h n}{c}\right) \tag{2.17}$$

From the equation 2.17, it is noted that the phase of the IF signal is linearly proportional to the step number (n) for a fixed distance (h). Applying the inverse discrete Fourier transform (IDFT) about n, generates an impulse signal. The position of the impulse peak determines the distance h to the target.

2.8 Digital Signal Processing

Digital signal processing is the manipulation of data using mathematical computations for processing raw data to meaningful information [11].

IQ Sampling A quadrature signal is a two-dimensional signal whose value at a point can be defined by a complex number with the real and imaginary part. Quadrature signals are also termed as complex signals and are commonly used in communication and radar systems [12]. The sine and cosine signals are in quadrature such that cos(x) = sin(x + 90°). Quadrature sampling or IQ sampling uses these signals mixed with the input signal to represent them as complex samples. The instantaneous amplitude and phase of the sample can be obtained from it.

Inverse Fourier Transform (IFT) The sampling points are extracted for each pulse. These are combined as a discrete sequence, and then IFT is performed to obtain the range profile. One arbitrary sampling point can be extracted in the time window of each pulse. The extracted data before the IFT can be expressed as

$$S_{\mathrm{IF}}(n) = \exp\left(-j\frac{4\pi f_0 h}{c} - j\frac{4\pi\Delta f h n}{c}\right) \tag{2.18}$$

Applying IFT for $S_{IF}(n)$ about n, the range profile is obtained as

$$S_r(n) = \mathrm{IFT}[S_{\mathrm{IF}}(n)] = \delta\left(n - \frac{2\Delta f h N}{c}\right) \cdot \exp\left(-j \cdot \frac{4\pi f_0 h}{c}\right) \tag{2.19}$$

where $\delta()$ is the impulse function in the discrete-time domain. Here $\frac{2\Delta f h N}{c}$ is assumed to be an integer. Not having an integer value is solved by upsampling using zero padding before performing IFT. The IFT of this spectrum gives the time domain signal for a sweep [5]. The time domain signals generated in multiple sweeps are compared for the phase and amplitude differences.

Inverse Fast Fourier Transform (IFFT) The time required to compute IFT depends on the mathematical computations like multiplications involved. Considering N as the length of the transform, N^2 is the number of multiplication operations involved in IFT. Avoiding the redundant multiplications involved in this, a faster method of computation was designed named as Inverse Fast Fourier Transform (IFFT) [13]. The IFFT for a frequency domain signal $X(k)$ can be expressed by equation 2.20.

$$x(n) = \frac{1}{N}\sum_{k=0}^{N-1} X(k) \cdot e^{j\frac{2\pi k n}{N}} \tag{2.20}$$

Here, $x(n)$ is the time domain signal and N is the number of sample points in the complex signal. The number of computations reduces from N^2 in IFT to $N\log(N)$ in IFFT.

3
Methods

The feasibility study of the stepped FMCW GWR was carried out in several steps. First step was to study current GWRs and identify the rationales for using a FMCW based GWR. Next, a literature review of FMCW technology in general and specific literature review on stepped FMCW radars was performed. An appropriate radar architecture was designed together with the microwave engineers considering factors like transmitted RF power, IF signal generation, etc. Most of the components used the hardware architecture were off-the-shelf evaluation boards. The MCU for the system was also selected at this stage considering the control interfaces, analog to digital converter (ADC) and processing capabilities.

The evaluation kits for the components selected were procured and interconnected using coaxial cables, SMA connectors and jumper wires to form the demonstrator setup. The circuits which were not available as evaluation kits were designed, simulated and finalized. The printed circuit boards were fabricated outside and components were assembled. The MCU software was developed and modifications on the architecture were done gradually based on individual component testing. The final architecture is confirmed and the measurement signal is acquired. This signal is transferred to PC and the advanced signal processing is done in MATLAB [14]. The radar was tested using coaxial cables of different lengths terminated by grounding to replicate the target. The power consumed by the circuit components in different configurations were measured and compared.

The desired resistive bridge as well as the IF filter and amplifier were not available to purchase as evaluation boards. So these circuits were designed, and simulated using LTSpice [15], a circuit simulator tool. The schematics and PCB for the resistive bridge, IF filter, and amplifier were designed using Kicad EDA [16] software. These PCBs were fabricated at Cogra Pro AB [17] PCB fabrication house. The components for the PCB were procured and assembled manually at Emerson.

The radar demonstrator consists of the evaluation kits and our custom PCAs. The microwave paths between the frequency synthesizers, mixers, RF switches, gain blocks, attenuator, resistive bridge and IF amplifier were connected using $50\,\Omega$ coaxial cables with SMA connectors. The control signals like SPI, I2C, UART, GPIO connections from the MCU to the different peripherals were connected via regular jumper wires.

A uniform transmitted power across the entire frequency range was assumed to help reproduce the echo curve with accuracy. Both the low frequency and high frequency synthesizers had output power control registers. The maximum power output was

set from the MCU and the output power with frequency steps of 10 MHz from 1 MHz to 4096 MHz were measured using a spectrum analyzer in dBm units and analyzed. A lookup table was created for attenuation based on the target transmission power in MCU firmware. Based on these values, the RF attenuator was controlled for each frequency step to maintain the uniform output power and the results were compared.

The IF signal generated using the down-converting mixer was checked and verified using an oscilloscope and a spectrum analyser for accurate frequency throughout the entire frequency sweep. After ensuring the proper IF signal reception, it was recorded using a digital oscilloscope and converted into a MATLAB data file (*.mat*) and imported to MATLAB, a programming and numeric computing platform. The IF signal samples in each frequency step were converted to the real and imaginary coefficients after IQ sampling multiplication and filtering in MATLAB. The $ifft$ function in MATLAB was used to compute the IFFT of the complex terms and derive the echo curve.

The IF signal was sampled using the inbuilt ADC of the MCU. The ADC resolution, sampling frequency and sample size per step were decided based on the choice of IF frequency. The amplitude and relative phase information for each step was recovered post sampling. The amplitude and phase information for each frequency step was transferred from the MCU to the PC serially. The amplitude and phase information were imported to MATLAB, modified and processed using IFFT to generate the echo curve to ensure proper sampling, amplitude and phase calculation by the MCU. But this proved to be not working as expected.

The IQ sampling alternative was tested in MATLAB using the oscilloscope sampled data. As this proved working, the same was implemented in the MCU and the complex coefficients were generated as DC components post low pass filtering. These were transferred to PC as before and IFFT was performed using MATLAB to verify. As this method proved working, the IFFT was implemented in the MCU and the echo curve data was generated from the MCU and transferred to the PC where the echo curve was plotted.

The measurement time, power consumption, accuracy, and other parameters were compared and analyzed to conclude.

4

Design

In this chapter, the design procedure, motivations and various design decisions of the FMCW GWR demonstrator are presented. The system architecture design is discussed first, followed by the individual component selections and their design. The software design and the signal processing techniques used in the work are also discussed in detail here.

4.1 Theoretical Simulation

The stepped FMCW concept was modelled in MATLAB and simulated. The circuit model is shown in figure 4.1. Here, $VCO1$ generates the transmitted frequency sweep expressed as S_{TX} and $VCO2$ generates the offset sweep expressed as LO with an offset Δf. S_{RX} is the reflected signal. It is mixed with LO to generate the IF signal. This is passed through the low-pass filter to isolate the IF_{LP} signal of Δf frequency.

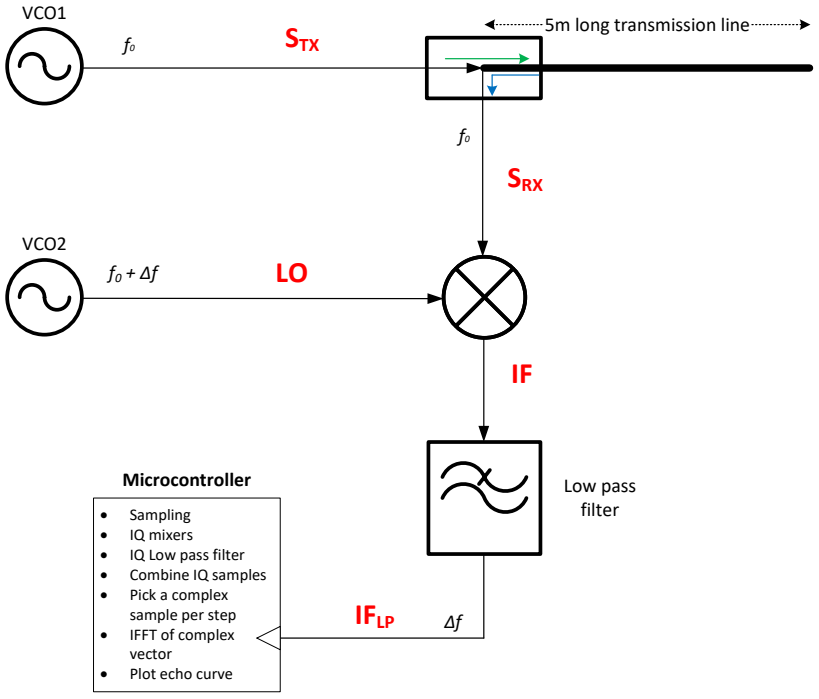

Figure 4.1: MATLAB model for Stepped FMCW simulation

The transmitted signal is mathematically expressed in equation 4.1 where ϕ_{f_0} is the initial phase of S_{TX}.

$$S_{TX} = \cos\left(2\pi f_0 t + \phi_{f_0}\right) \tag{4.1}$$

The reflected signal is mathematically expressed in equation 4.2.

$$S_{RX} = S_{TX} \cos\left(\frac{2\pi}{\lambda} \cdot 2R\right) \tag{4.2}$$

where R is the range of the target and λ is the wavelength.

The local oscillator (LO) signal is expressed in equation 4.3.

$$LO = \cos\left(2\pi f_1 t + \phi_{f_1}\right) \tag{4.3}$$

where

$$f_1 = f_0 + \Delta f \tag{4.4}$$

The IF signal is expressed in equation 4.5.

$$IF = S_{RX} \cdot LO \tag{4.5}$$

After passing through a low-pass filter of cutoff 1.2 times the offset frequency, the IF signal can be expressed as equation 4.6.

$$IF_{LPF} = LPF_{f_cutoff=1.2\Delta f}(IF) \tag{4.6}$$

When expanding, we get as below.

$$IF_{LPF} = \frac{1}{2} \cos\left(\frac{2\pi}{\lambda} \cdot 2R\right) \cos\left(2\pi\Delta f t + \phi_{f_0} - \phi_{f_1}\right) \tag{4.7}$$

The complex frequency sweep obtained after Inphase/ Quadrature (IQ) demodulation can be expressed as equation 4.8.

$$C = I + jQ = \frac{1}{4} \cos\left(\frac{2\pi}{\lambda} 2R\right) \left[\cos(\phi_{f_0} - \phi_{f_1}) + j \sin(\phi_{f_0} - \phi_{f_1})\right] \tag{4.8}$$

The phase difference between the two VCOs is $\phi_{f_0} - \phi_{f_1}$. If the phases are uncorrelated, $\phi_{f_0} - \phi_{f_1}$ becomes random and we cannot detect the range R whereas if ϕ_{f_0} and ϕ_{f_1} are fully correlated, $\phi_{f_0} - \phi_{f_1}$ becomes zero and C only contains the range information R. This is expressed as below.

$$C = I + jQ = \frac{1}{4} \cos\left(\frac{2\pi}{\lambda} 2R\right) \tag{4.9}$$

Figure 4.2 shows the echo curves for different phase difference values for the VCOs in stepped FMCW model. This proves the need for a correlated phase at each step for both the VCOs.

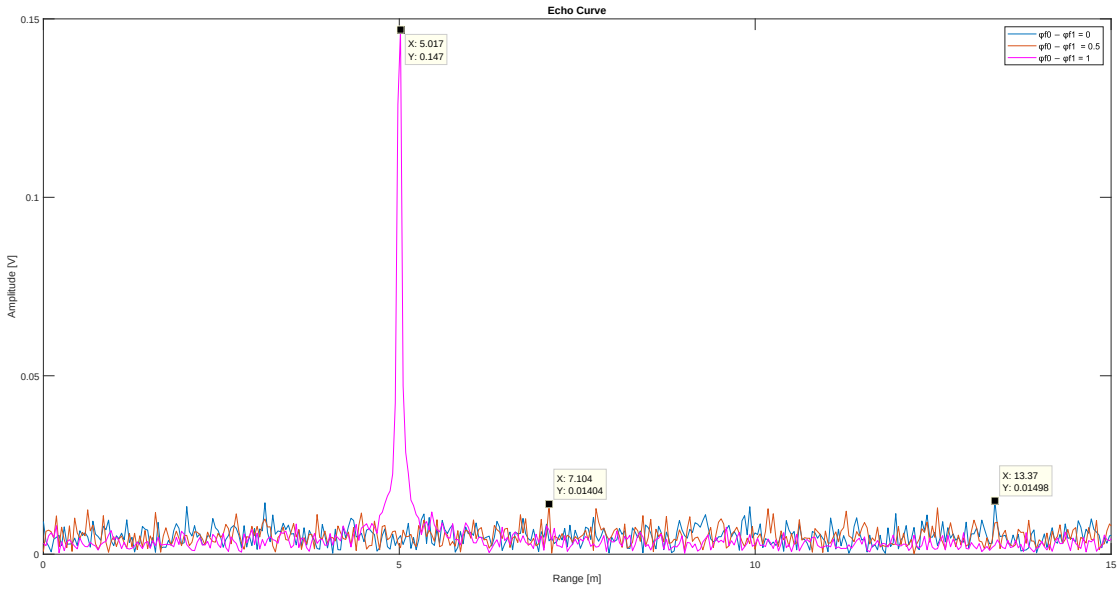

Figure 4.2: Echo curve for different phase constants in Stepped FMCW model simulation

4.2 Radar Architecture

Figure 4.3 shows the radar architecture designed as part of the thesis for the stepped FMCW demonstrator. As Emerson wants to protect the details of the actual circuit due to confidentiality, we consider that there are two separate VCOs for both the low-frequency (LF) and high-frequency (HF) synthesizers.

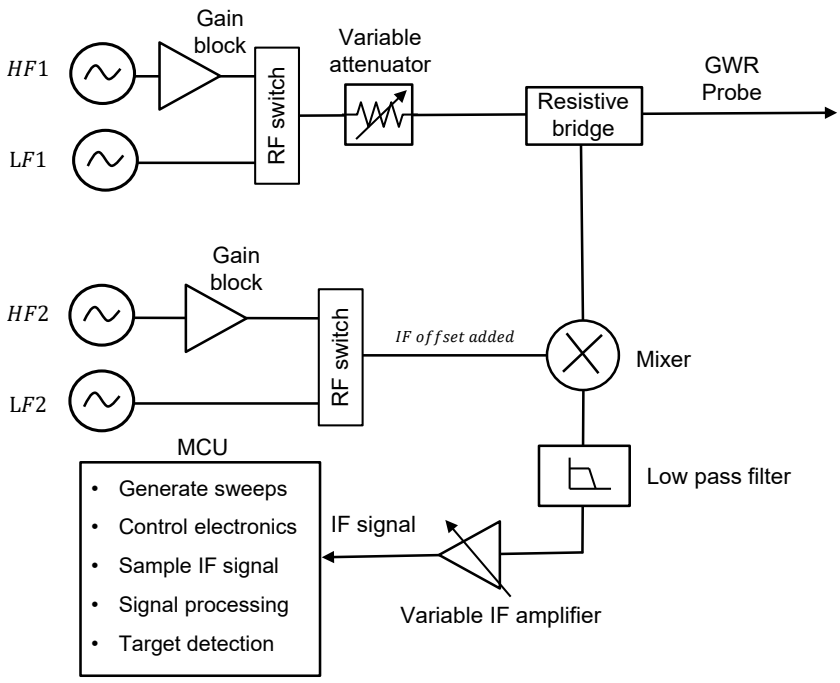

Figure 4.3: Stepped FMCW radar system architecture

The microwave circuit consists of a HF synthesizer, LF synthesizer, gain blocks, variable attenuator, RF switches, mixer, and a resistive bridge. A single frequency synthesizer could not cover the desired frequency range from 1 MHz to 4 GHz. Therefore, two separate frequency synthesizers were used. VCO-based PLL was used for the higher frequencies and a VCXO-based PLL for the lower frequencies. But the concern was on the unrelated phase between the sweep frequency and the offset frequency being produced by two unrelated VCOs. It is necessary to maintain a correlated phase for both the mixer inputs. Both of these synthesizers do not generate clean sinusoidal waves as they generate each frequency signal using multiple levels of frequency dividers. So, we cannot generate the phase and amplitude response by mixing the transmitted and reflected signals. This called for the generation of an offset frequency sweep using the same source as the transmitted signal generating an IF signal. This also results in variable power levels for different frequencies. This motivated us to use a variable attenuator that can be controlled by the MCU, along with a gain block, helping in maintaining a usable power level for the entire frequency range from 1 MHz to 4 GHz.

The resistive bridge is used to direct the synthesized frequency signal from the PLL to the transmission line and also to direct the reflected signal to the mixer to generate the IF signal. The mixer is used for generating the IF frequency from the reflected signal. As this signal will have the impact from the high frequency harmonics, a low-pass filter is used to segregate the 10 kHz IF signal, which is sampled by the ADC inside the MCU. The IF signal varies in amplitude based on the RF echo from the tank. An IF amplifier circuit with gain varied using an MCU controlled potentiometer is used to obtain a good IF signal within ADC thresholds which can be properly sampled by the ADC.

RF switches are used to switch between the multiple channels of the two frequency synthesizers to direct the correct frequency to the transmission line as well as its offset while the frequency sweeps from 1 MHz to 4 GHz. The RF switch and the gain block showed variations in their performance for lower frequencies. The gain block failed to amplify the frequencies upto a certain MHz range and the RF switch applied an attenuation of near 20 dB for these frequencies. Also, the ADL5611 [18] gain block was measured to be attenuating low frequencies like 1 MHz to 5 MHz and providing gain only upto 11.29 dB for frequencies upto 20 MHz. The ADL5611 gain block was restricted to the HF synthesizer only in the transmission side to avoid the attenuation of low frequency signals. On the path to upmixer, another 14.5 dB gain block part TRF37B73 [19] was introduced to satisfy the minimum power requirement for the mixer, since we observed that the HF synthesizer power is very low at some frequencies.

4.3 RF Synthesizers

The RF signals transmitted and received through the GWR have to be generated using a special electronic circuit. The total bandwidth of the FMCW sweep is the first parameter in the design of this section.

4.3.1 RF Bandwidth Requirement

The accuracy of a target range with FMCW radar is determined by the range resolution, which in turn depends on the bandwidth of the radar waveform. A wider bandwidth leads to higher range resolution, and bandwidth depends on the waveform generated by the oscillator. However, an oscillator with a wide bandwidth incurs high costs [20]. In FMCW sweep, the theoretical range resolution for a radar system can be calculated [21] as

$$\delta r = \frac{c}{2B} \tag{4.10}$$

where c is the speed of electromagnetic wave in air and B is the bandwidth. The actual range resolution in the existing pulsed GWRs like Emerson Rosemount 3300 and 5300 is about 100 mm corresponding to 1.5 GHz bandwidth. They have an accuracy of 3 mm achieved by further interpolation [10]. In our stepped FMCW, the targetted bandwidth is 4 GHz which gives a resolution of 37.5 mm as per equation 4.10.

4.3.2 Selection Of Start And Stop Frequencies

The maximum measuring range for Emerson Rosemount 5300 GWR is 50 m [10]. The lowest frequency of the sweep define the maximum measuring range as shown below.

$$R_{\max} = \frac{c}{2 \times f_{min}} \tag{4.11}$$

The maximum range is given by the step size not the minimum transmitted frequency. The phase can't change more than π (real sampling) or 2π (complex sampling) for each step.

$$\Delta f = \frac{c}{4 \cdot d_{\max}} \tag{4.12}$$

or

$$\Delta f = \frac{c}{2 \cdot d_{\max}} \tag{4.13}$$

The 1 MHz starting frequency is selected because it gives 150 m range. Also, 1 MHz step frequency will give 4000 samples up to 4 GHz. We can select a different start frequency like 5 MHz, step with 5MHz and end in 2 GHz if we want a fast measurement. 5 MHz will give 30 m distance which is enough for most applications in GWR.

4.3.3 RF Synthesizer Part Selection

Analog frequency synthesizer with inbuilt PLL and VCO components was selected due to their lower cost compared to digital frequency synthesizers. Table 4.1 lists a selection of wide band frequency synthesizers suitable for our application. The minimum and maximum frequency thresholds (f_{min} and f_{max}), power consumption for a channel (P_{1ch}) and the cost are added for comparison. As we can see, none of these components can synthesize frequencies over our complete desired range from 1 MHz to 4 GHz. Therefore, another frequency synthesizer was required at lower

Table 4.1: Frequency synthesizer options at higher frequencies

Sl#	Mfg	Part	P_{1ch} (mW)	f_{min} (MHz)	f_{max} (MHz)	Cost ($)
1	TI	LMX2581E	587.4	50	3800	5.8
2	ADI	ADF4351BCPZ	369.6	35	4400	9.18
3	ADI	ADF4350BCPZ	369.6	137.5	4400	7.77
4	STM	STW81200T	528	46.875	6000	9.52
5	Renesas	8V97051NLGI	501.6	34.375	4400	6.68
6	Microchip	MAX3674ECM2	396	21.25	1360	14.7
7	ADI	MAX2871ETJ+	544.5	23.5	6000	8.99

frequencies. So, to generate the lower frequencies upto 1 MHz, there was the need for a different synthesizer.

The off-the-shelf components supporting the low frequency synthesis are listed in table 4.2. The minimum and maximum frequency thresholds f_{min} and f_{max}, power consumption for a channel P_{1ch} and the cost are added for comparison. It was

Table 4.2: Frequency synthesizer options at lower frequencies

Sl#	Mfg	Part	P_{1ch} (mW)	f_{min} (MHz)	f_{max} (MHz)	Cost ($)
1	TI	LMX2571NJKT	168.3	10	1344	9.11
2	ADI	ADF4360-9BCPZ	100.65	1.1	200	3.78
3	Infineon	CY22394FXI	330	0	166	8.54
4	Infineon	CY223931FXI	330	0	166	23.02
5	TI	CDCE913QPWRQ1	19.8	0.078	230	2.98
6	Skyworks	SI5351B-B-GM1	148.5	0.025	200	2.63

decided to use two separate frequency synthesizers to cover the entire sweep range from 1 MHz to 4 GHz. Based on the availability of the evaluation boards inhouse, ADI part ADF4351BCPZ [22] was selected for the higher frequency range generation and Skyworks SI5351B-B-GM1 [23] for the lower frequency range.

AD4351 is a VCO-based PLL chip supporting frequencies from 35 MHz to 4.4 GHz [22]. The integrated VCO has a fundamental output frequency ranging from 2200 MHz to 4400 MHz. The divide-by-1/-2/-4/-8/-16/-32/-64 circuits allow the user to generate RF output frequencies as low as 35 MHz. AD4351 has a primary output and an auxiliary output. The internal registers for the frequency setting and other controls are accessed via 3-wire serial interface which is compatible with SPI.

Si5351B is a VCXO-based PLL chip consisting of two PLLs - PLLA and PLLB. Each PLL generates an intermediate VCO frequency in the range of 600 MHz to 900 MHz. These VCO frequencies can then be divided down by individual output multisynth dividers to generate any frequency between 500 kHz and 200 MHz. Multisynth is a low jitter fractional divider that supports phase error correction. Additionally, the R dividers can be used to generate any output frequency down to 2.5 kHz. The

relationship between the VCO frequency (f_{vco}), multisynth divider (M_d), multisynth feedback divider (M_f), R divider (R) and output frequency (f_{out}) is

$$f_{out} = \frac{f_{vco}}{M_d \cdot R} \tag{4.14}$$

where

$$f_{vco} = f_{in} \cdot M_f \tag{4.15}$$

The internal registers for the frequency setting and other controls can be accessed via I2C serial interface.

4.4 Transmit Power

The RF signals generated using the ADF4351 and SI5351B-B frequency synthesizers were found to differ much in the power with the change in frequency. The lower frequencies had higher power output, whereas the higher frequencies had very low power output mostly due to the presence of multiple divider stages following the VCO stage. This variation in power affects the reflected power from the target which thereby influence the IF signal sampled.

For ADF4351, the primary RF output $RFOUTA+$ and the auxillary output are connected to the collectors of an NPN differential pair driven by buffered outputs of the VCO. The tail current of the differential pair is programmable using bits $[DB4 : DB3]$ in Register 4 (R4) of the chip. Four current levels can be set giving output power levels of -4 dBm, -1 dBm, +2 dBm, and +5 dBm, using a 50 Ω resistor to Analog power supply (AVDD) and ac coupling into a 50 Ω load [22]. So, the output power can be controlled by only the four different values shown above with the SPI interface connected to the MCU for this synthesizer.

For SI5351B-B, there are $CLKx$_IDRV$[1 : 0]$ 2-bit registers where x varies from 0 to 7 for all the eight clock outputs from $CLK0$ to $CLK7$ [24]. The output power can be configured in drive current to values 2 mA, 4 mA, 6 mA, and 8 mA by updating these bits corresponding to each clock register. So, the output power can be controlled by only the four different values shown above with the I2C interface connected to the MCU for this synthesizer. The output power for both the low frequency and high frequency synthesizers were measured using a RS FSP-40 spectrum analyzer. The measurements were made at the resistive bridge connector to the transmission line. The power was measured from 1 MHz to 4101 MHz in 10 MHz steps and is plotted in figure 4.4. We observed random fluctuations in power due to the standing waves. This was cleared by the use of a 10 dB attenuator which is also shown in the second graph in figure 4.4. The python script used to control the spectrum analyzer to sweep from 1 MHz to 4101 MHz and measure the transmit power is shown in appendix A.1.

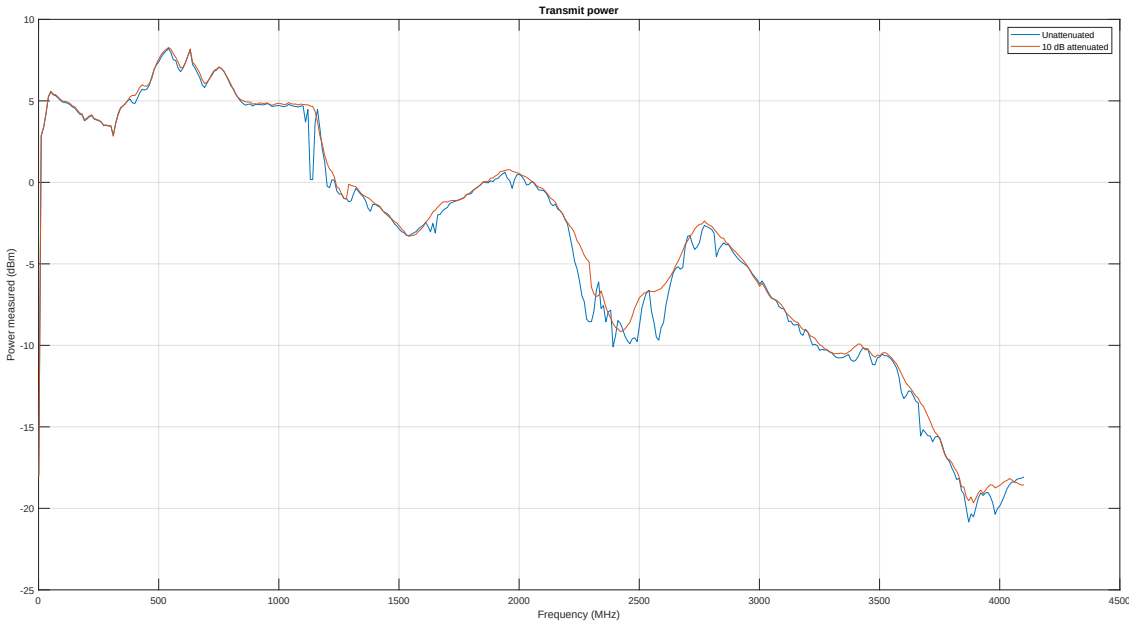

Figure 4.4: Transmit power measured at the resistive bridge

4.4.1 Ensuring Constant Transmit Power

An RF gain block, and a programmable RF attenuator external to the frequency synthesizers control the output transmitted power. The RF gain block is expected to provide a constant gain to all different frequency signals in its supported range which brings them to a level suitable for transmission. This power can then be regulated using the RF attenuator by different values to maintain a constant power being transmitted to the GWR probe at all frequencies. But we observed that gain varies much based on the frequency in practice. The ADL5611 RF/IF Gain block supports frequencies from 30 MHz to 6 GHz gives an average 22.2 dB gain which could bring the least powered signal to 12 dBm which is sufficient for the application. HMC472ALP4E is a digital attenuator chip that supports attenuation values from 0.5 dB to 31.5 dB controllable in 0.5 dB units. The control is via six CMOS control inputs which are driven by the MCU. The TRF37B73 is another RF gain block which offers 14.5 dB gain working from 1 MHz to 6 GHz. It was added in the HF offset path to the mixer. To ensure uniform power across the entire frequency range, HMC472ALP4E attenuator was added in HF signal path which can attenuate the signal in 0.5 dB units from 0.5 dB to 31.5 dB.

4.5 Resistive Bridge

A resistive bridge circuit was designed to separate the reflected echo from the transmitted signal. A balun transformer was used to convert the echo to a single ended signal referenced to ground. The circuit for the resistive bridge is shown in figure 4.5.

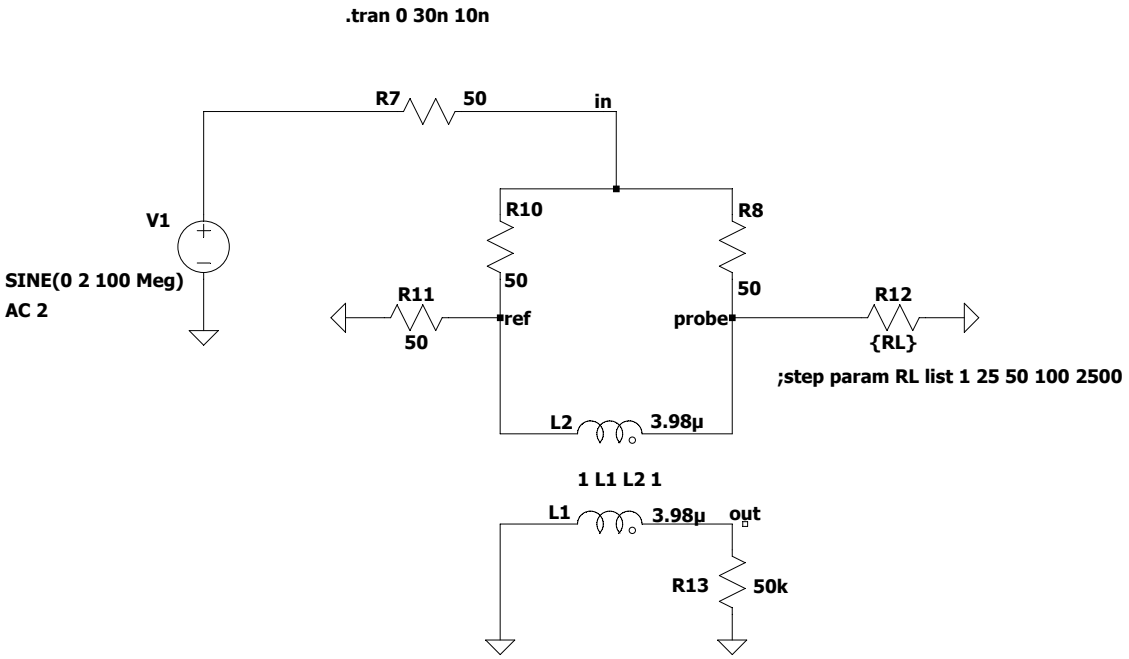

Figure 4.5: Circuit for resistive bridge

The transmitted signal is depicted by the source $V2$. $R12$ shows the GWR probe. $L1$ - $L2$ shows the balun transformer. The transformer coil inductance is chosen for 100 MHz reference frequency using equation 4.16.

$$L = \frac{R_s \times R_L}{2\pi f} \tag{4.16}$$

The PCB designed for the resistive bridge circuit is shown in figure 4.6. RFF_Tx shows the input port for the transmitted signal from the frequency synthesizers. GWR Probe shows the port to connect the GWR probe and RF_Rx shows the port for the reflected echo to the down mixer generating the IF.

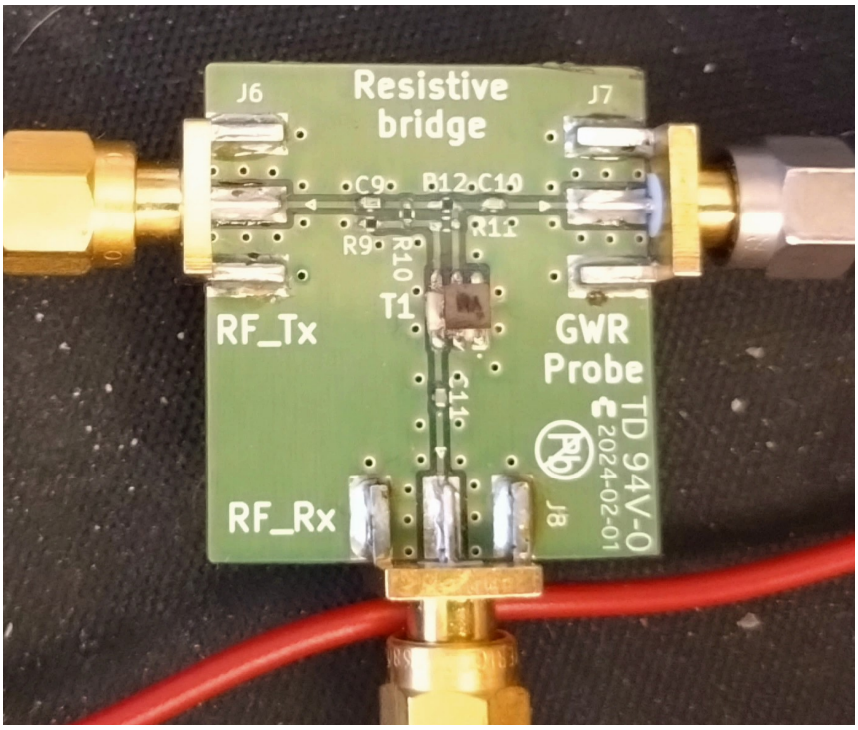

Figure 4.6: Resistive bridge PCB

The node *out* shows the point of reflected echo measurement. Figure 4.7 shows the plot of the response during simulation. The input signal $V(in)$, signal transmitted to probe $V(probe)$ and the reflected echo signal $V(out)$ are shown in it. The attenuation in the input signal when passed through the bridge and still lower reflected signal is visible in it. The reflected signal amplitude was found okay for sampling by ADC.

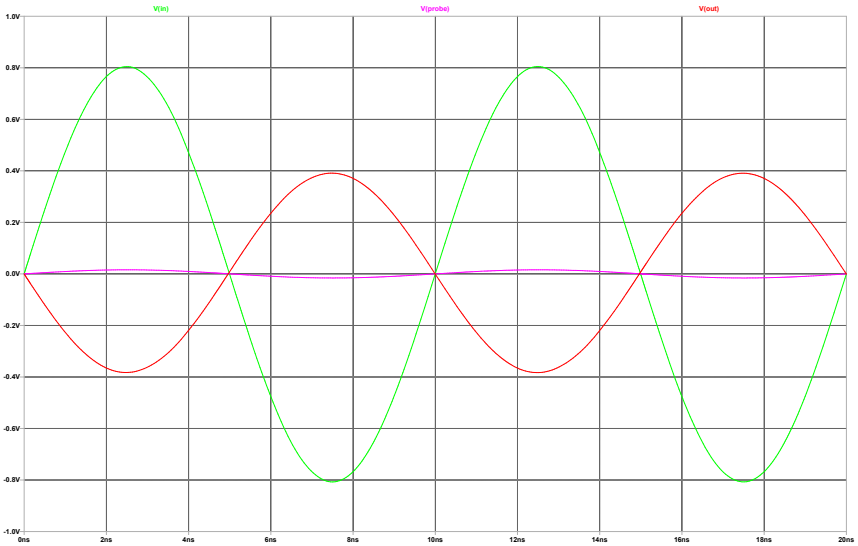

Figure 4.7: Circuit simulation for resistive bridge

4.6 IF Signal Generation

The reflected echo has to be sampled to digital signal to generate the frequency spectrum for the sweep. This signal should have the amplitude and phase response for each frequency step. The frequency synthesizers are not capable of generating a clean sinusoidal waveform and has harmonics. Figure 4.8 shows the spectra for a 10 MHz signal generated using the LF synthesizer. We can see the odd harmonics in 30 MHz, 50 MHz, etc of decreasing amplitude.

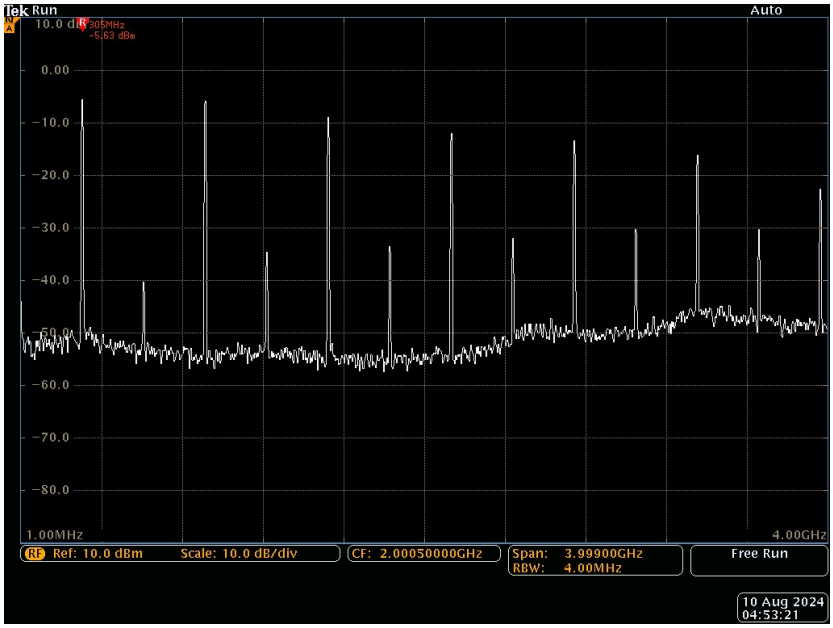

Figure 4.8: Frequency spectrum for 305 MHz generated from HF synthesizer

In figure 4.9, we can see the spectra of 305 MHz frequency signal generated by the HF synthesizer. It also has the odd harmonics in 915 MHz, 1525 MHz, etc of more uniform amplitude.

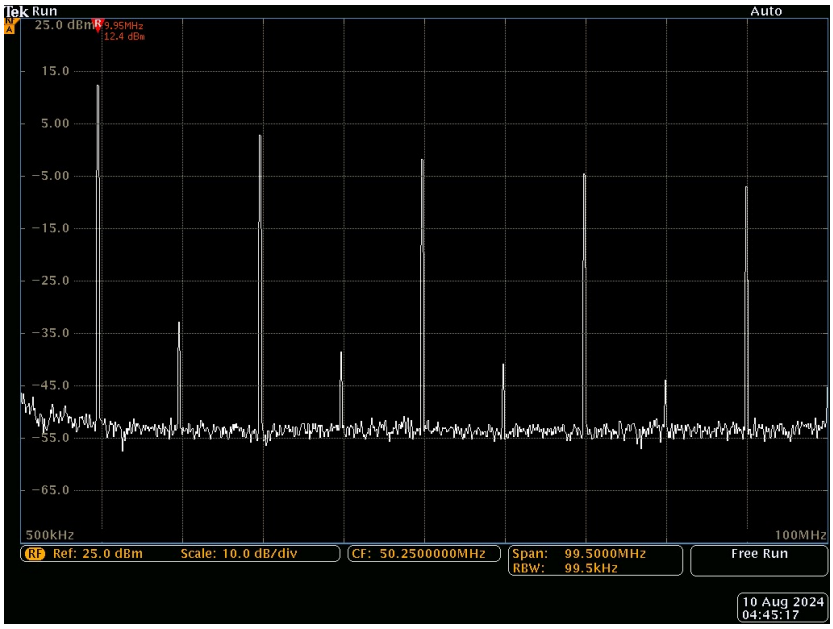

Figure 4.9: Frequency spectrum for 10 MHz generated from LF synthesizer

The inbuilt ADC of the low power MCUs have ADCs with sampling rates of few mega samples per second (MSps). The IF signal frequency to be sampled by the ADC was decided to be 10 kHz. This 10 kHz offset added to the sweep frequency was transmitted through a second channel. This is applied to the RF mixer at the local oscillator (LO) input, and the reflected echo from the target at the RF input. As the mixer generates the difference of two frequencies, we get a 10 kHz IF signal at the IF output port for sampling as shown in figure 4.10.

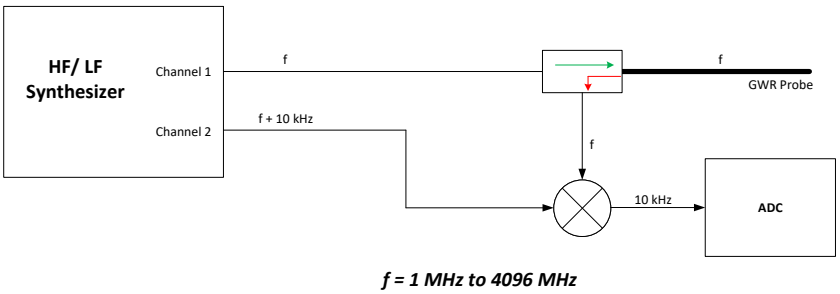

Figure 4.10: Scheme of IF generation

AD8342 [25] is the active mixer used to generate the IF. HMC544AE SPDT switches controlled with CMOS control inputs from the MCU were used to route the RF signals.

4.7 Compensating For The Electronics In Received IF Signal

The received IF signal will be sampled and used for amplitude and phase. As the reflected signal travels from the target to the directional coupler and then through the mixer, the amplitude of the signal will be affected by losses which could be different based on frequency. So, an IF amplifier and filter circuit is added to compensate for these losses. The received power at the directional coupler after reflection at the target can be expressed as equation 4.17.

$$P_{\mathrm{RX}} = P_{\mathrm{TX}} - 2A_eR + r - 2L_{\mathrm{seal}} \tag{4.17}$$

where P_{RX} is the received power, P_{TX} is the transmitted power, A_e is the attenuation coefficient of the transmission line, R is the distance to the target, L_{seal} is the loss across the seal. Further, the power of the IF signal to be sampled at the ADC can be expressed as

$$P_{\mathrm{IF}} = P_{\mathrm{RX}} - L_e \tag{4.18}$$

where P_{IF} is the power of the IF signal and L_e is the loss across the electronics including the resistive bridge, and mixer. The signal to noise ratio (SNR) for the IF signal is expressed as

$$SNR_{IF} = P_{IF} - N_P \tag{4.19}$$

where N_P is the noise power. A common assumption of the minimum SNR required for proper target detection $\mathrm{SNR_{IF}}$ is 6 dB.

4.7.1 Amplifier And Filter Circuit

The IF signal is amplified using an opamp circuit. The signal is also filtered to remove the harmonics to the fundamental 10 kHz IF signal. The schematics of the circuit designed is shown in figure 4.11. AD8544 general purpose opamp is the active element used in the circuit. Two opamps among the four available in the package are used in the filter circuit. A second order low-pass filter of 15 kHz cutoff frequency is designed. Differential output from the mixer denoted as in and in_neg is input to the filter which gives a single ended output $filter\_out$. One opamp is used as an emitter follower to create half of the power supply voltage vcc which is termed as vcc_half. The fourth opamp is used as the inverting amplifier. The biasing point for this amplifier is set as vcc_half. The gain is controlled by the resistors $R2$ and $R5$.

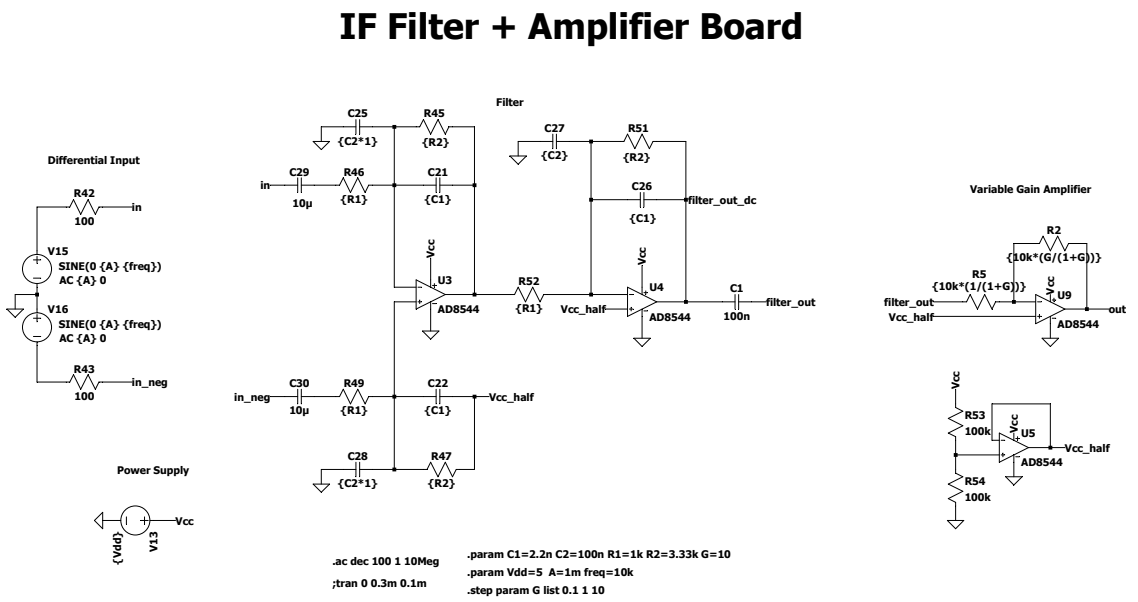

Figure 4.11: IF amplifier and filter circuit

The image of the PCB designed is shown in figure 4.12. The banana jack connectors are used to input the 3.3 V DC power input to the board. The IF output is taken from the 2-pin header marked as $Vout$. The 3-pin header marked as $J3$ has the A, W and B terminals for the potentiometer marked. These replace $R2$ and $R5$ resistors in the schematics.

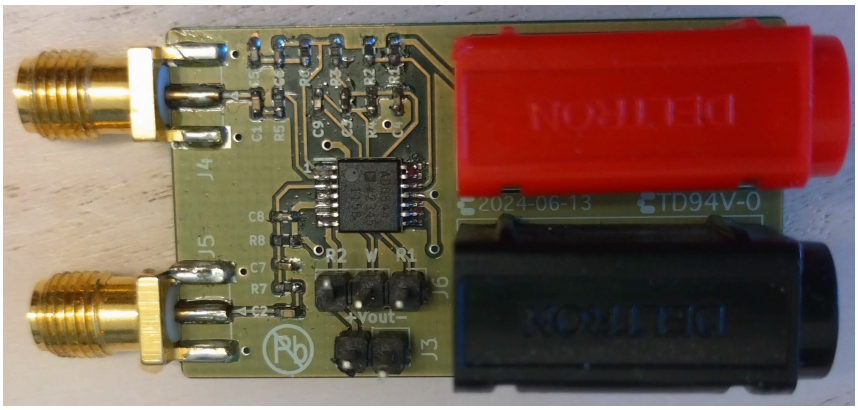

Figure 4.12: IF amplifier and filter PCB

The simulation results for the AC response of the amplifier and filter circuit is shown in figure 4.13. We use a 1 mVpp 10 kHz differential sinusoidal input through $V15$ and $V16$ for the simulation. $vout/(vin - vin\_neg)$ shows the amplified output waveform and $filter\_out$ shows the filtered output of the low-pass filter.

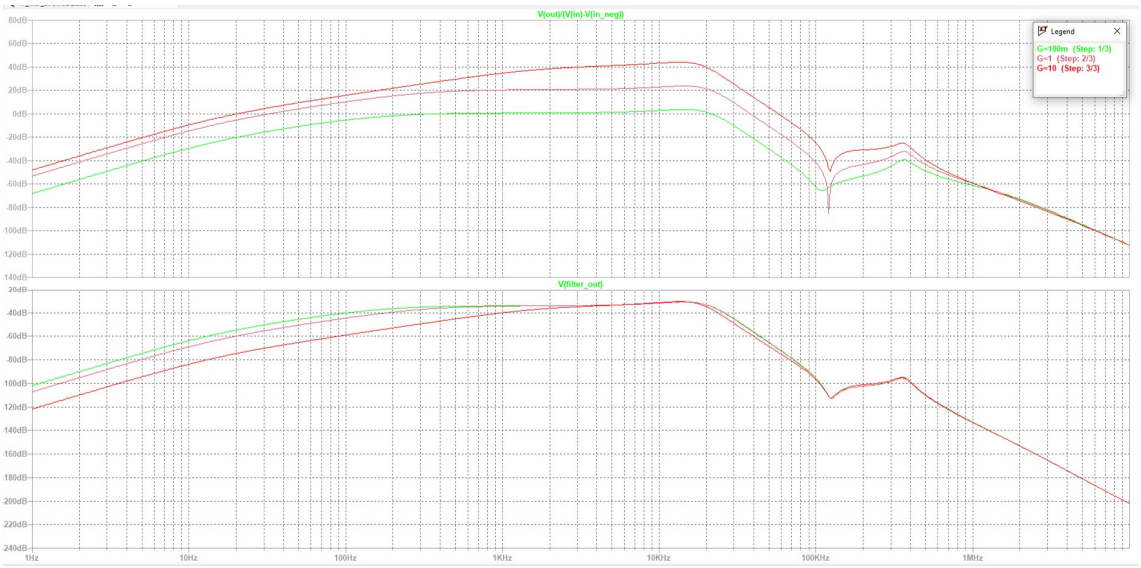

Figure 4.13: AC simulation for IF amplifier and filter circuit

Gain Control For Amplifier

The gain of the amplifier is controlled by varying the $R2$ and $R5$ resistor values in the schematic shown in figure 4.11. This is done using a digital PMOD potentiometer module with 10 kΩ AD5160 SPI compatible digital potentiometer IC. AD5160 is a SPI-compatible digital potentiometer with 8-bit resolution and can be controlled by an MCU. $R2$ was connected between the W and B terminals and $R5$ was connected between A and W terminals. The resistance between A and B terminals was 10 kΩ. An 8-bit register controls the position of W terminal and the value 0 being written to it gets 0 Ω between A and W and 10 kΩ between W and B. On the other hand, a value 255 written to this register gets 10 kΩ between A and W and 0 Ω between W and B. We wrote 128 to the register to get around 5 kΩ between A and W and another 5 kΩ between W and B. This gave a unity gain through the variable gain amplifier.

4.8 Control Circuit

The STM32U575 MCU is used as the heart of the design as shown in figure 4.14. It interface the low and high frequency synthesizers via I2C and SPI serial interfaces. The RF switches and the RF attenuator are controlled using general purpose IOs (GPIO) and the digital potentiometer using another SPI interface. The universal asynchronous receive and transmit [UART) interface helps in transferring the processed data to the computer for analysis. The inbuilt ADC of the MCU samples the IF signal.

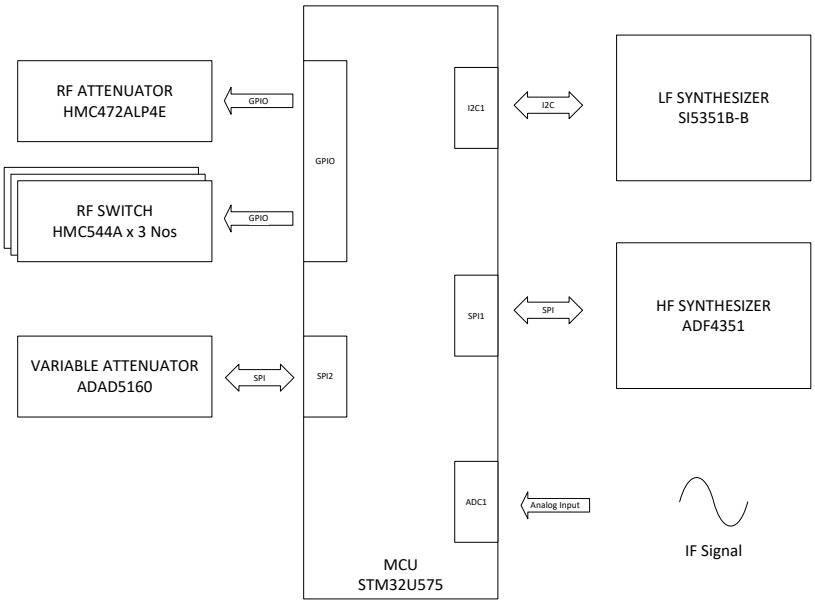

Figure 4.14: MCU interface with peripherals

4.9 Software Design

This section describes the software design of the demonstrator. It includes the control interfaces as well as the signal processing involved.

4.9.1 Sweep Generation

The frequency sweep is generated by controlling the frequency synthesizers via serial interfaces. The flow chart of the sweep generation scheme from 1 MHz to 4096 MHz is shown in figure 4.15. This is a loop which checks for frequency value and enables the LF and HF synthesizers accordingly. The LF synthesizer has $CLK0$, $CLK1$, and $CLK2$ channels which are being controlled, whereas the HF synthesizer has the $CLK+$ and $CLK-$ channels being controlled. After reaching the maximum frequency of 4096 MHz, both the synthesizers are powered down.

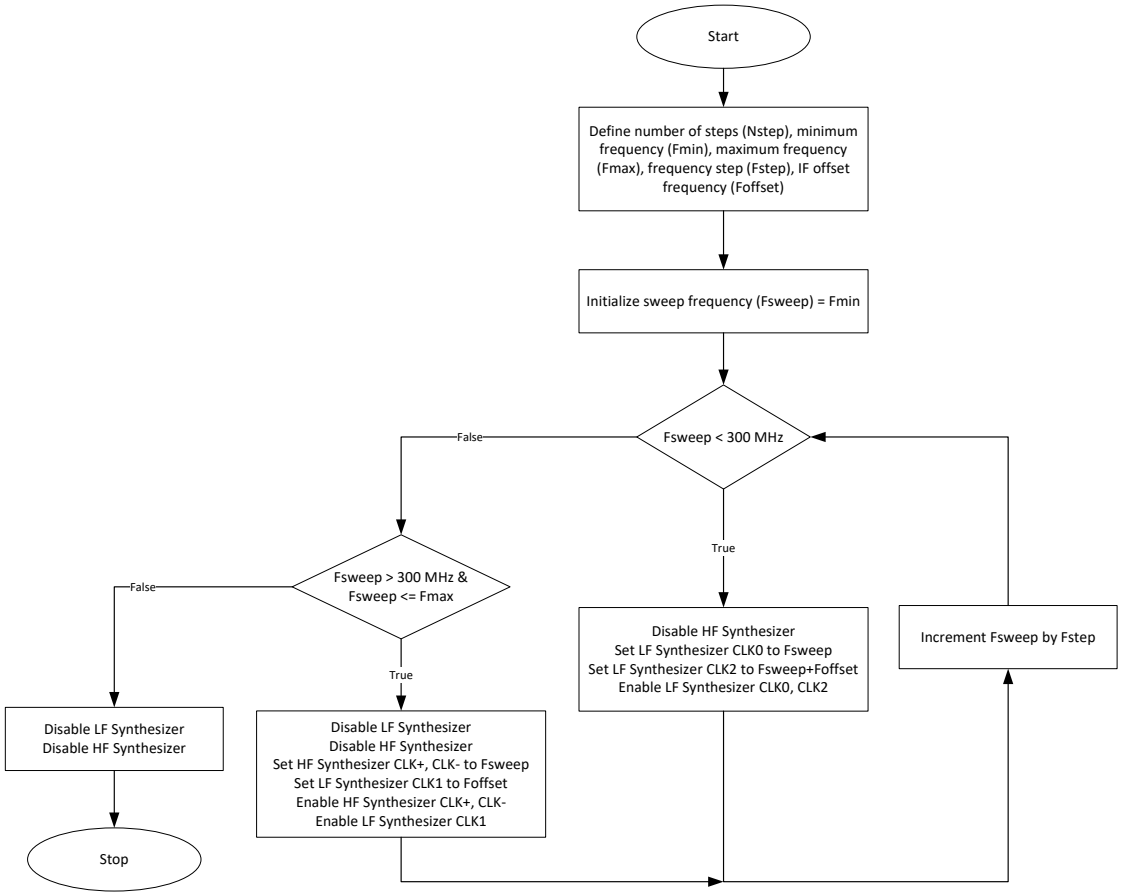

Figure 4.15: Flowchart of sweep generation

4.9.2 Transmit Power Control

The transmit power control in software is initiated by creating a lookup table for attenuation values to be applied for each step from 1 MHz to 4096 MHz. This is stored as an array *att_data*[4096] with 4096 elements. As the attenuator control is via 6 IOs, we use an 8 bit integer value for the attenuation values. Writing a 0 gives the maximum attenuation of 31.5 dB, whereas a 63 gives minimum of 0 dB attenuation. The flow chart of the software is shown in figure 4.16. At each frequency step, before enabling the synthesizer output, the attenuator is initialized with the concerned value.

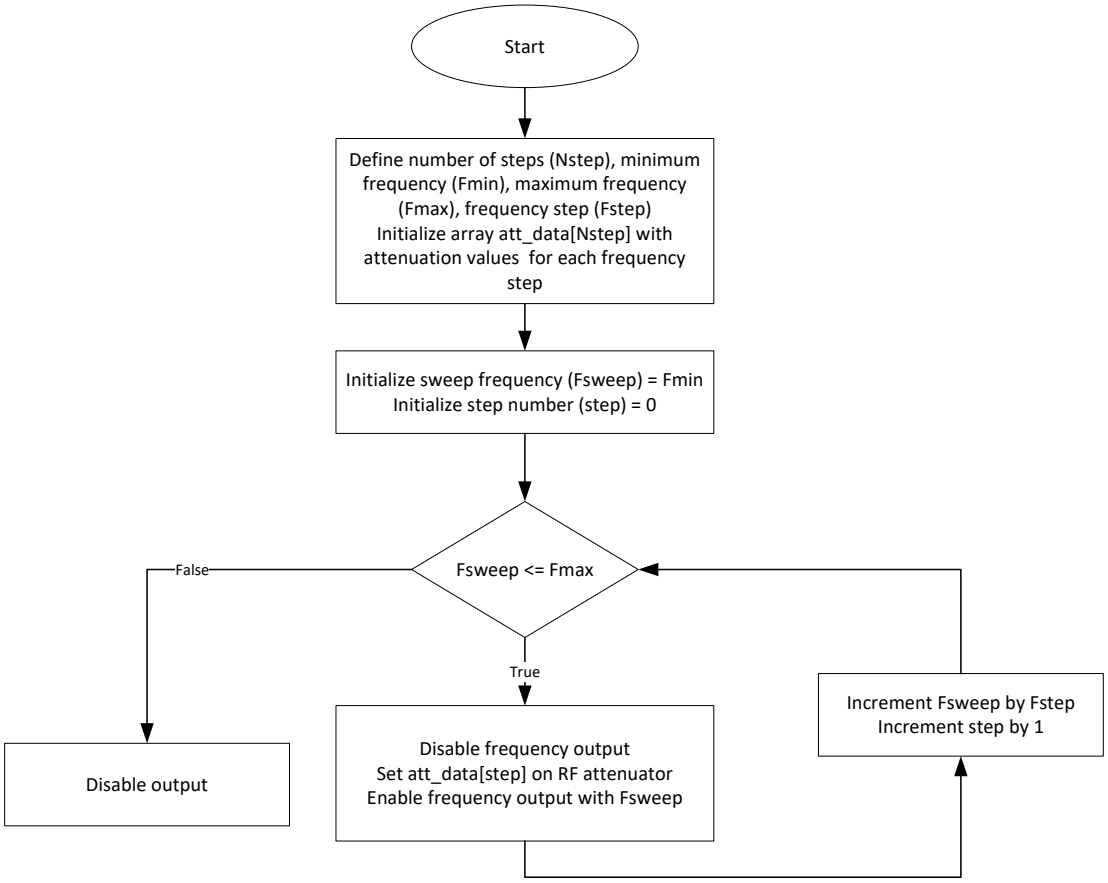

Figure 4.16: Flowchart of transmit power control

4.9.3 Sampling Of IF Signal By ADC

The 14-bit ADC1 peripheral of STM32U575 is used for sampling the IF signals. Channel 16 of it is used in continuous conversion single ended mode for it. We decided to use 4 samples per frequency step to sample a full cycle of the 10 kHz IF signal. This calculates to an effective conversion frequency requirement of 40 kHz per sample. This is a total conversion time of 0.025 ms per sample. The ADC was configured for 391 cycles for sampling. As 17 cycles are needed for conversion, it requires 408 cycles per sample. To get the target 40 kHz effective sampling frequency, the cycle time was set to 61.3 ps by configuring the ADC prescalar divider to 1 and setting the internal ADC clock frequency to 16.32 MHz. The flowchart of the sampling process for IF signal in the sweep is shown in figure 4.17.

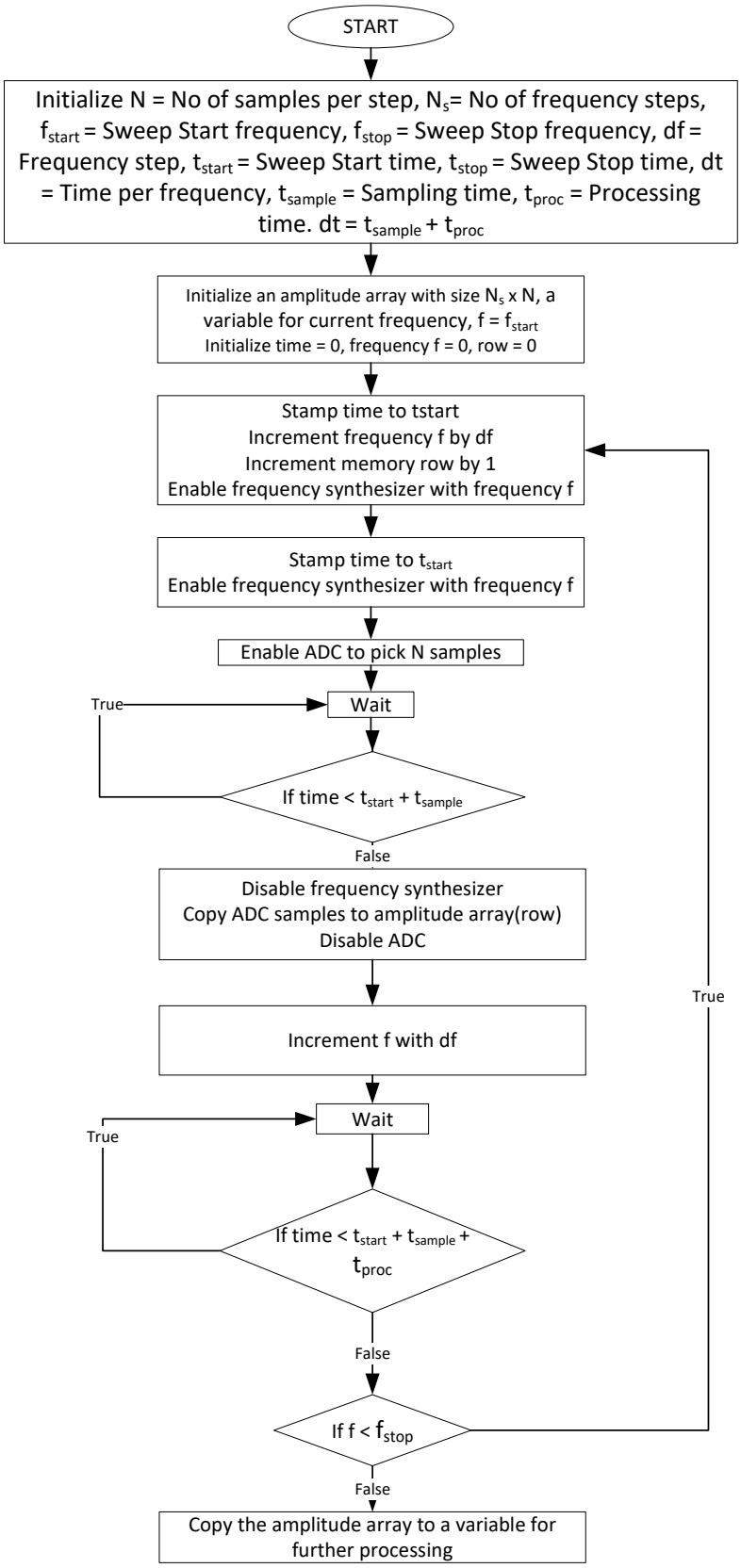

Figure 4.17: Flowchart of sampling by ADC

4.9.4 IQ Sampling

The sampled signals are multiplied by sinuous and cosinuous waveforms of the IF frequency to derive the inphase and quadrature components of sampled data.

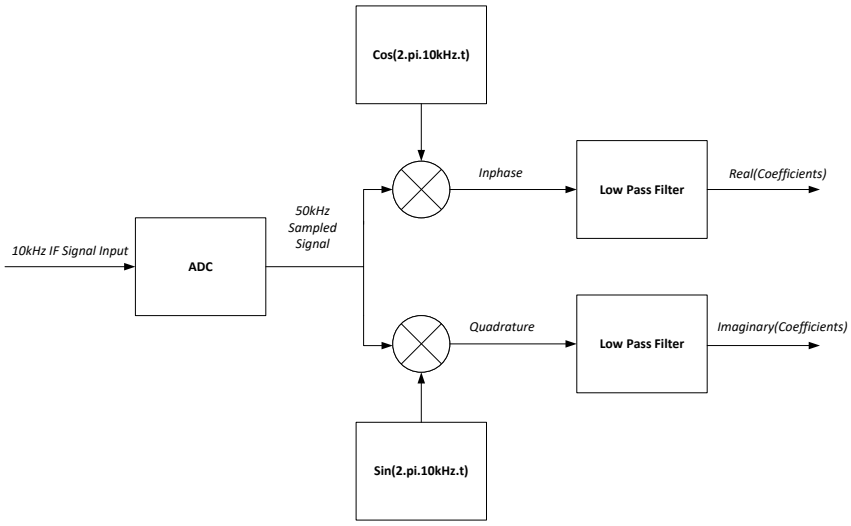

Figure 4.18: Block diagram of IQ sampling

4.9.5 Filtering

The IQ sampled signals are passed through a low-pass filter of 100 Hz cutoff frequency to derive the DC part of the inphase and quadrature components. We also tried averaging the coefficients than a filter for performance comparison.

Averaging Of Samples

The mean of all the samples is calculated separately for both the inphase and quadrature components, and are used as the real and imaginary coefficients of the complex signal for the IFFT. We sampled the 10 kHz signal using 40 kHz sampling frequency. By taking 4 samples, we covered a full signal cycle per frequency step. As we took 4 samples in every frequency step, we calculated the average of the 4 inphase coefficients and used it as real part of the complex sample. Similarly, we calculated the average for the 4 quadrature coefficients and used it as the imaginary part of the complex sample prior to performing IFFT.

FIR Low-pass Filter

The filter initialization function was declared as below.

```
void arm_fir_init_f32(arm_fir_instance_f32 *S,
                      uint16_t numTaps,
                      const float32_t *pCoeffs,
                      float32_t *pState,
                      uint32_t blockSize );
```

Here, S points to an instance of the floating-point FIR filter structure, $numTaps$ define the number of coefficients in the filter, $pCoeffs$ points to the filter coefficients buffer, $pState$ points to the state buffer and $blockSize$ defines the number of samples processed per call. We designed a 6th order FIR filter in MATLAB using Window-based FIR filter design function $b = fir1(n, Wn)$ where n is the filter order and Wn is the cutoff frequency. b gave the 6 filter coefficients which are applied to $pCoeffs$. We used 4 as the block size and 6 as the number of taps. The filter response is plotted in figure 4.19. An attenuation of more than 15 dB is visible for frequencies above 10 kHz and more than 30 dB for 15 kHz which align with our requirements.

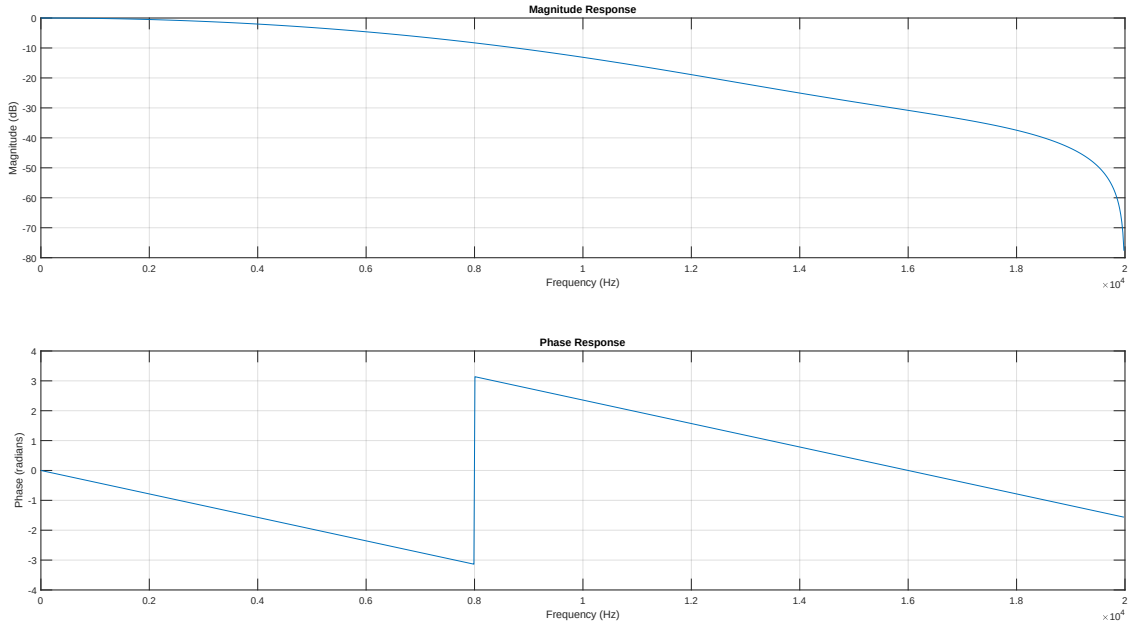

Figure 4.19: Amplitude and phase response for FIR low-pass filter

The processing function for the filter was declared as below.

```
void arm_fir_f32( const arm_fir_instance_f32 *S,
                  const float32_t *pSrc,
                  const float32_t *pCoeffs,
                  float32_t *pDst,
                  int32_t blockSize );
```

Here, S points to an instance of the floating-point FIR filter structure, $pSrc$ points to the block of input data, $pDst$ points to the block of output data, and $blockSize$ defines the number of samples to process. We used 4 as the block size as we take 4 samples per step, thereby giving 4 element array as the input and output for both the inphase and the quadrature coefficients.

For comparison, echo curves were generated for the same target employing FIR low-pass filter and the averaging method post IQ sampling as shown in figure 4.20. The target was a 10.07 m coaxial cable shorted to ground at the end. The FIR filter gave an SNR of 18 dB whereas the averaging gave 16 dB.

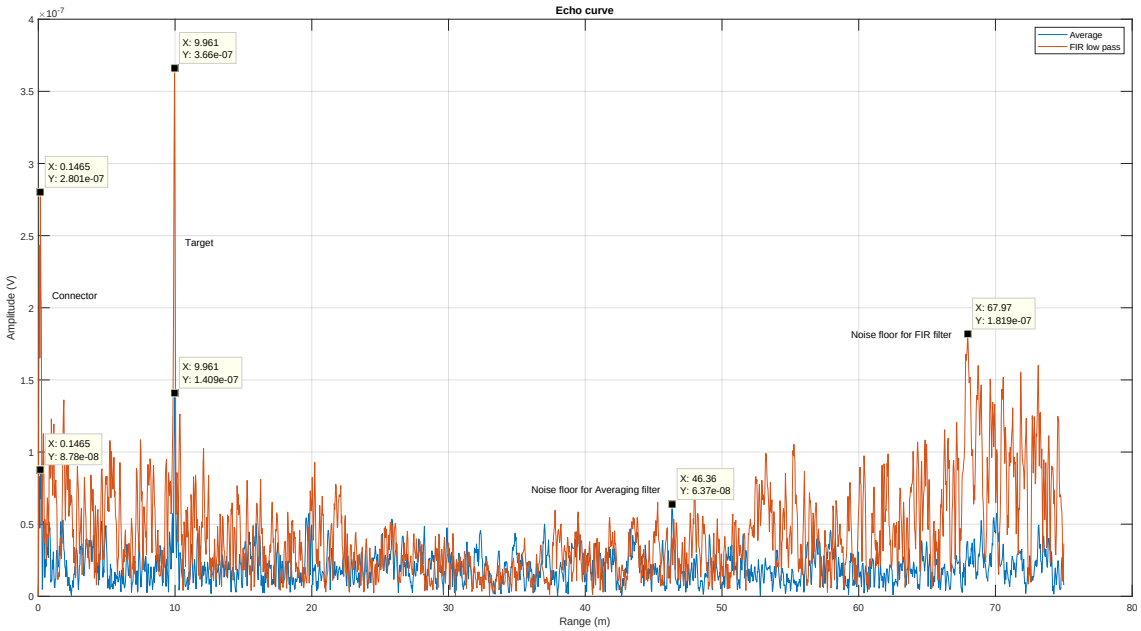

Figure 4.20: Comparison of echo curve for 10.07 m target employing different low-pass filters

4.9.6 Inverse Fast Fourier Transform

The FFT is simplest if the length of samples is an integral power of 2. The CMSIS DSP software library [26] with signal processing functions for use on Cortex-M and Cortex-A processor-based devices is also designed for the same. So, we increased the sample size from 4000 to 4096 before applying the IFFT function. The Complex Fast Fourier Transform (CFFT) function available is used for it. *arm_cfft_instance_f32* is an instance structure for the floating point IFFT function used from CMSIS library.

```
arm_status arm_cfft_init_f32 ( arm_cfft_instance_f32 *S,
                               uint16_t fftLen )
```

is the initialization function for the transform. S points to an instance of the floating-point CFFT structure. We use the instance that we initialized before for this. $fftLen$ input is the length of the complex input samples which is 4096 in our case. The return variable *arm_status* is compared in a loop to expected *ARM_MATH_SUCCESS* to confirm that the operation is completed.

```
void arm_cfft_f32( const arm_cfft_instance_f32 *S,
                   float32_t *p1,
                   uint8_t ifftFlag,
                   uint8_t bitReverseFlag )
```

is the CFFT function performing the inverse transform of the complex inputs. S points to the same instance of floating-point CFFT structure as before. $p1$ points to the complex input buffer which is double the size of $fftLen$. The input buffer is of 8192 size with the real and imaginary parts of the 4096 complex input samples which are stored interleaved. The processed output is also recovered as interleaved from

this location. $ifftFlag$ input selects between forward and inverse transform options. We set it as 1 for selecting the inverse transform function. Bit reversal of the output is enabled by setting the $bitReverseFlag$ variable to 1. Each output sample is scaled by dividing it with the FFT size of 4096. The absolute value of each complex sample is calculated and transferred serially to PC. The UART communication port which is part of the Stlink interface is used for it. 500 kbps is the transfer rate used. These 4096 absolute values of amplitudes are plotted against the range in x-axis. For the maximum frequency of 4096 MHz, the range resolution is 0.0367 m.

5

Experimental Results

The chapter contains the results collected from the stepped FMCW demonstrator.

5.1 Frequency Sweep

The power output of both the frequency synthesizers are shown in figure 5.1. The power from 1 MHz to 300 MHz generated by the LF synthesizer is nearly constant, whereas in the case of HF synthesizer, it varies much with frequency. So, we used the gain blocks only for the HF synthesizer path. Both the LF and HF synthesizers were configured in maximum drive strength for the measurements. The second graph with gain block shows that both the synthesizers have comparable power outputs.

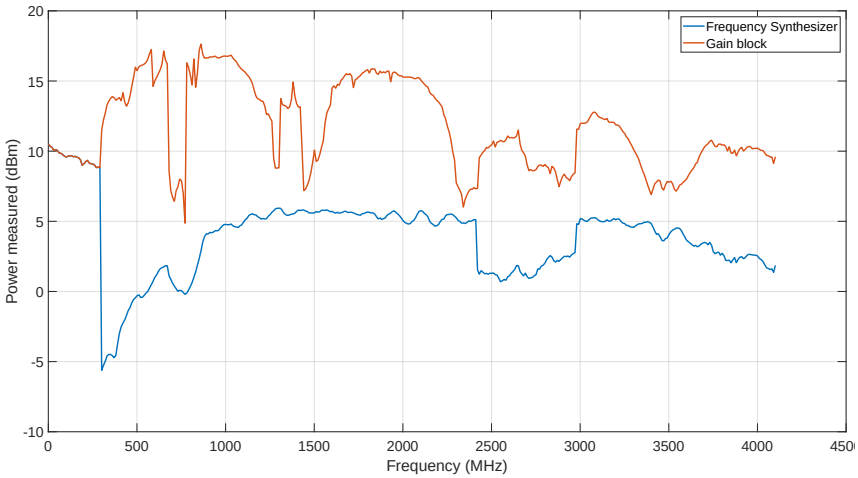

Figure 5.1: Power output of the frequency synthesizers prior to and after amplification

The transmit power was measured at different stages in the circuit and plotted in figure 5.2.

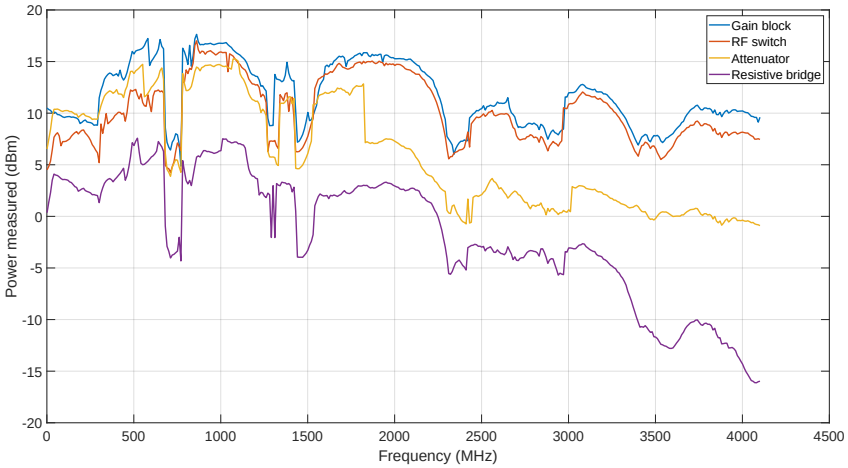

Figure 5.2: Power of the transmitted signal measured at different circuit stages

The attenuation applied by the RF switch is also evident. Following 3 GHz, the attenuation in the resistive bridge is higher than expected. This calls for an improved resistive bridge PCB design with proper electromagnetic (EM) simulation in future. To find the reflected power from the target, we measured the received power output of the resistive bridge connecting coaxial cables of different lengths terminated by ground. This is shown in figure 5.3.

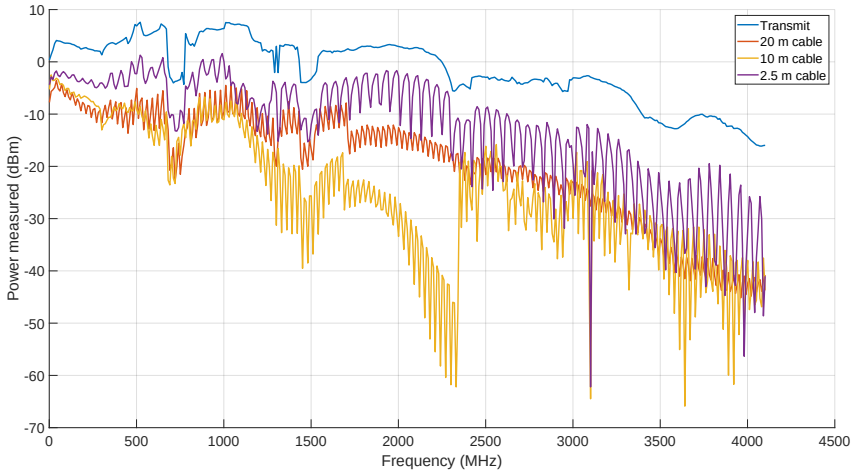

Figure 5.3: Reflected power measured for coaxial cables of different lengths with grounded ends

5.2 IF Signal Output From Low-pass Filter And Amplifier

The LF synthesizer takes away more time compared to the HF synthesizer to generate the PLL lock at each step. This is due to the delay in the I2C read process in checking for the lock in an internal register. I2C is run in the standard mode of 100 kHz clock frequency. So, the frequency steps from 1 MHz to 300 MHz are slow,

whereas the HF synthesizer has a dedicated Lock Detect (LD) GPIO pin. This read operation is very quick such that the sweep from 301 MHz to 4 GHz finishes fast. The entire sweep recorded using a high resolution oscilloscope named PicoScope is shown in figure 5.4.

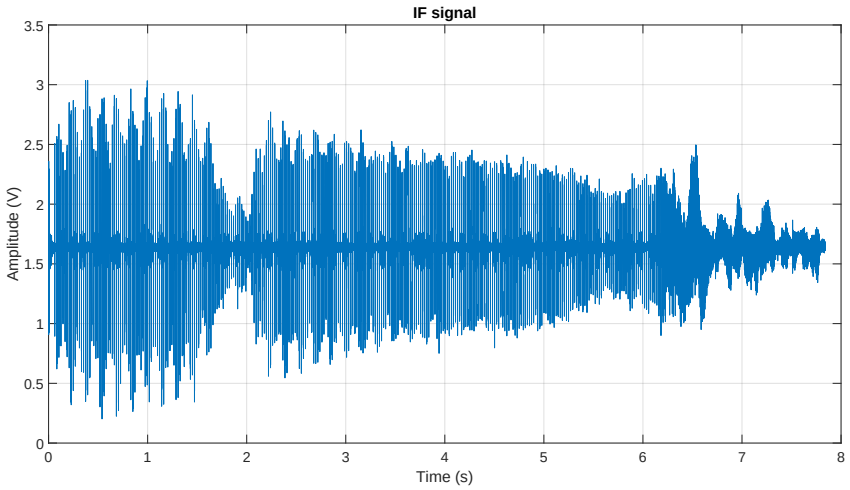

Figure 5.4: IF signal received for the frequency sweep from 1 MHz to 4096 MHz in 1 MHz steps

5.3 Sampled IF Signal At ADC

The IF signal of 10 kHz was sampled at a rate of 40 kS/s. Four samples were taken in each step giving a total of 16384 samples for the 4096 steps as shown in figure 5.5.

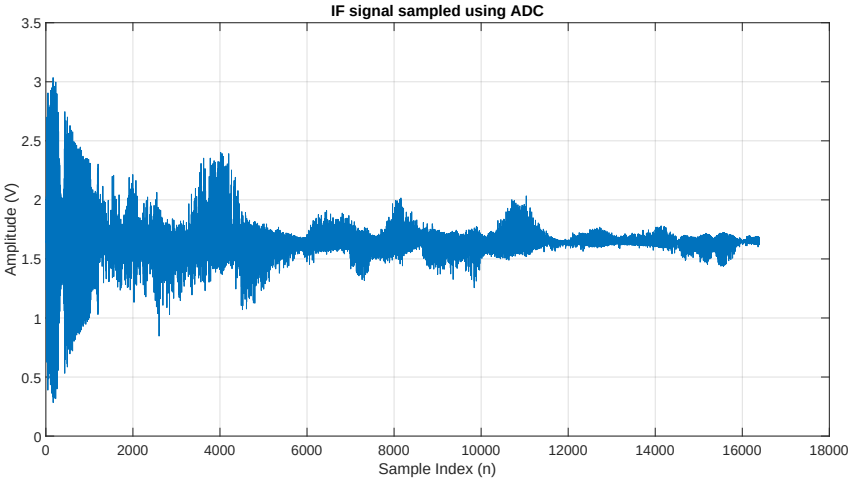

Figure 5.5: Sampled signal at the ADC of the MCU

The samples are normalized in amplitude before further processing as shown in figure 5.6.

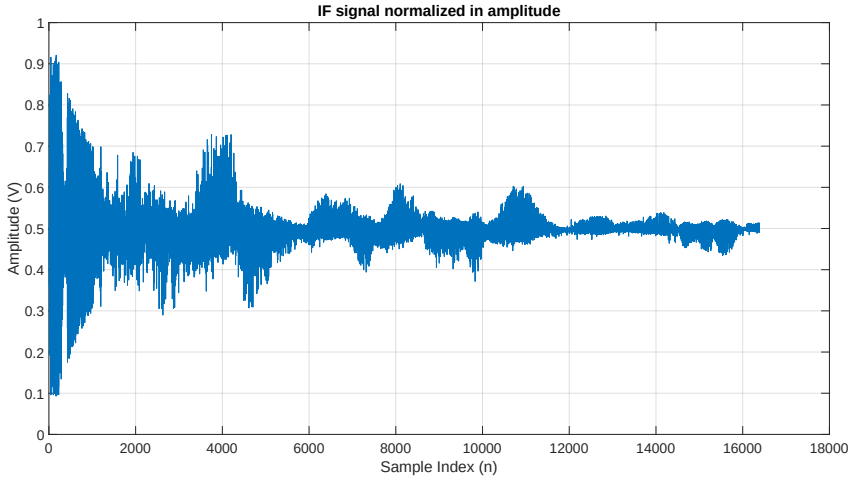

Figure 5.6: Samples normalized in amplitude

5.4 Inphase And Quadrature Component Generation

The samples at each frequency step from 1 MHz to 4 GHz are multiplied by the 10 kHz sinusoidal and cosinusoidal samples generated internally by the MCU. The inphase (I) and quadrature (Q) components generated are shown in figure 5.7.

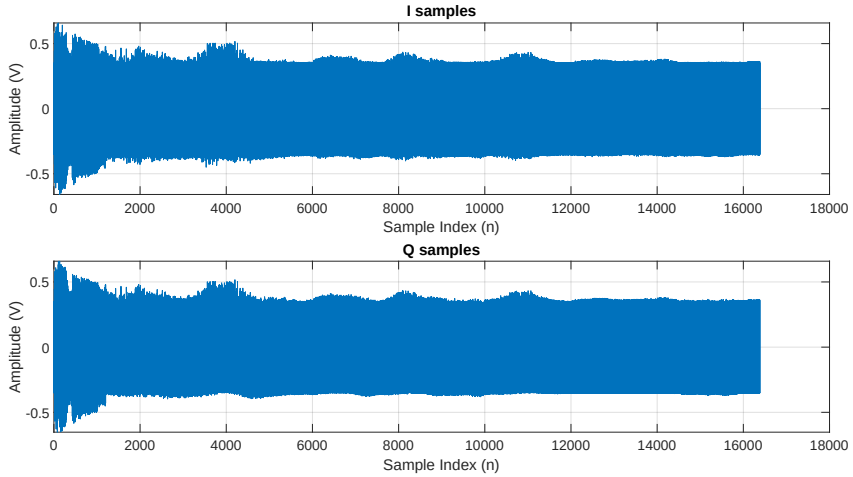

Figure 5.7: Inphase and quadrature components

The normalized samples have amplitudes between 0 V and 1 V, whereas the sinusoidal functions has amplitude between 1 V and -1 V. So, the multiplication for IQ sampling gives IQ components between 1 V and -1 V.

5.5 Low-pass Filtering Of IQ Samples

The impact of low pass filtering on the IQ samples is shown in figure 5.8.

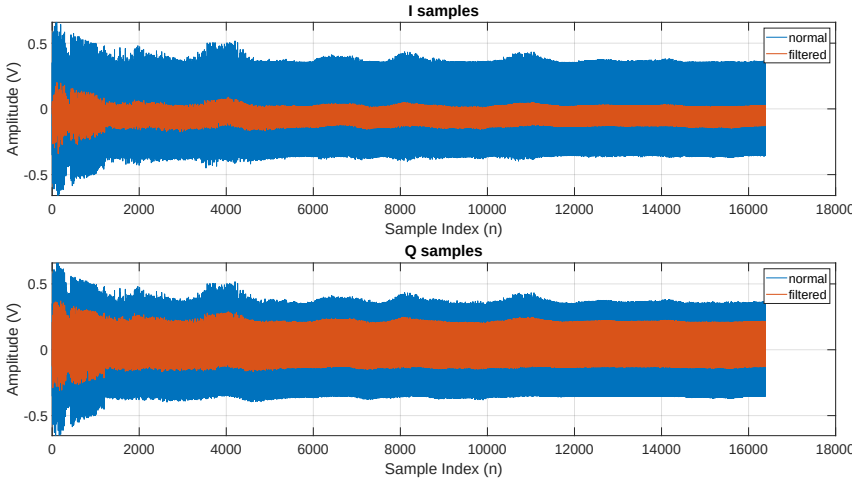

Figure 5.8: Impact of low pass filtering on IQ samples

We can see that the amplitudes for the higher frequency steps are very low due to the attenuation in the received signal.

5.6 Deriving Complex Coefficients

The real and complex coefficients for the complex samples were generated by using both FIR low pass filter as well as by averaging of samples. These were compared and the performance of the FIR filter was found to be better. Figure 5.9 compare the coefficients generated by both methods.

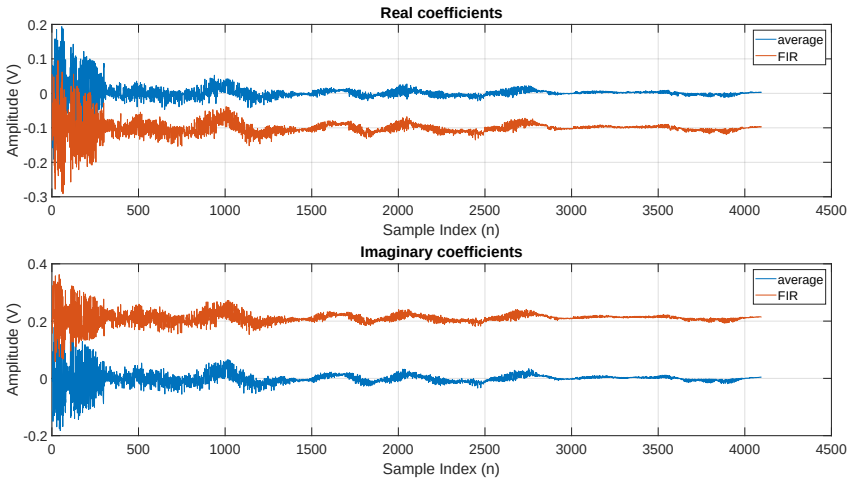

Figure 5.9: Real and imaginary coefficients generated

5.7 Echo Curve And Peak Detection

Figure 5.10 shows the echo curve obtained for 20 m coaxial cable with grounded end at a bandwidth of 4096 MHz. The reflection from the coaxial cable connector

as well as that from the grounded end are visible. The range is calculated as the difference between them, which is 19.4437 m. The SNR is 12.58 dB for the echo curve generated using average filter whereas it is 14.56 dB for the one created using FIR filter.

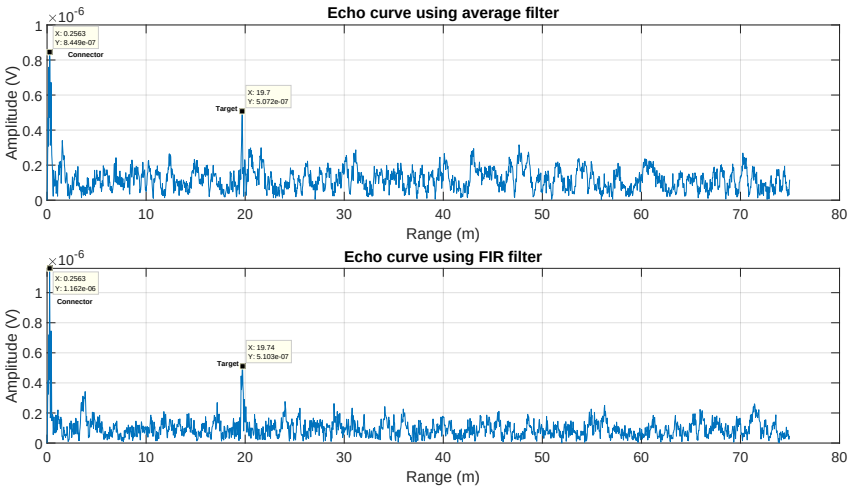

Figure 5.10: Echo curve for 20 m coaxial cable with grounded end

5.8 Measurement Time

The time for one measurement in the existing Emerson pulsed GWR is less than 100 ms.

In our stepped FMCW demonstrator, the total time for a measurement is 9.334 s. Figure 5.11 shows that the system initialize at 0 s, sweep starts from 1 MHz at 61.1 ms. The frequency sweep stops at 4096 MHz in 7.848 s and after signal processing and data transfer, the measurement completes in 9.334 s. The second plot in the figure is an IO indicating the software flow.

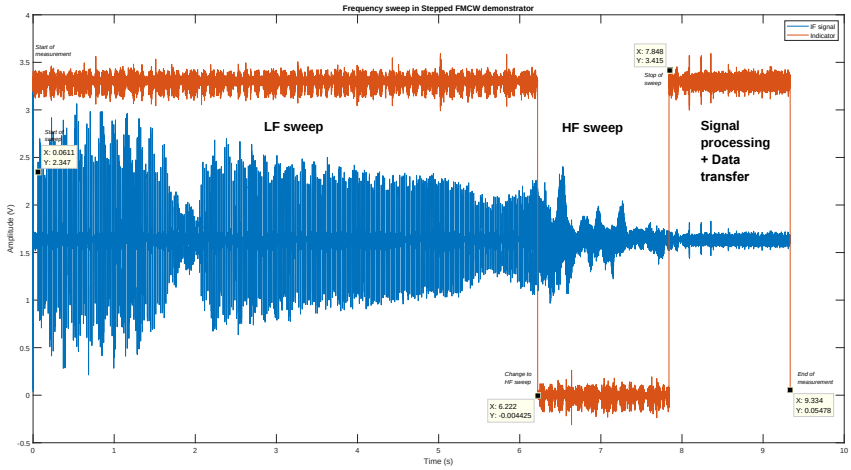

Figure 5.11: IF Signal recorded across the entire sweep from 1 MHz to 4096 MHz in 1 MHz steps

The LF sweep ends at 300 MHz in 6.222 s which count the LF sweep time as 6.161 s, whereas the HF sweep stops at 7.848 s counting to 1.626 s to sweep from 301 MHz to 4096 MHz. The reason behind this slow sweep for the LF synthesizer is the software check for PLL lock via I2C interface running on 100 kHz clock frequency, whereas the HF synthesizer has a dedicated output pin which responds faster.

5.9 Power Consumption

For Emerson pulsed GWR, the average power consumption is 28.32 mW and 29.14 mW is the maximum. The consolidated power consumption for the stepped FMCW demonstrator is shown in table 5.1. It is very high compared to the pulsed radar as we measure the total power consumed by the evaluation boards.

Activity	**System Power Consumption**
Radar Idle	1.51 W
Low Frequency Sweep	1.53 W
High Frequency Sweep	1.90 W
MCU Data Processing And Transfer	1.51 W
Radar In Reset	1.49 W

Table 5.1: Consolidated power consumption of the radar

5.10 Tank measurements

The radar demonstrator was tested in 3.1 m water pipes with various level configurations. Figure 5.12 shows the echo curve obtained for a water level of 100 cm and an ullage of 3 m. The measurement was done with a rigid probe and a standard seal.

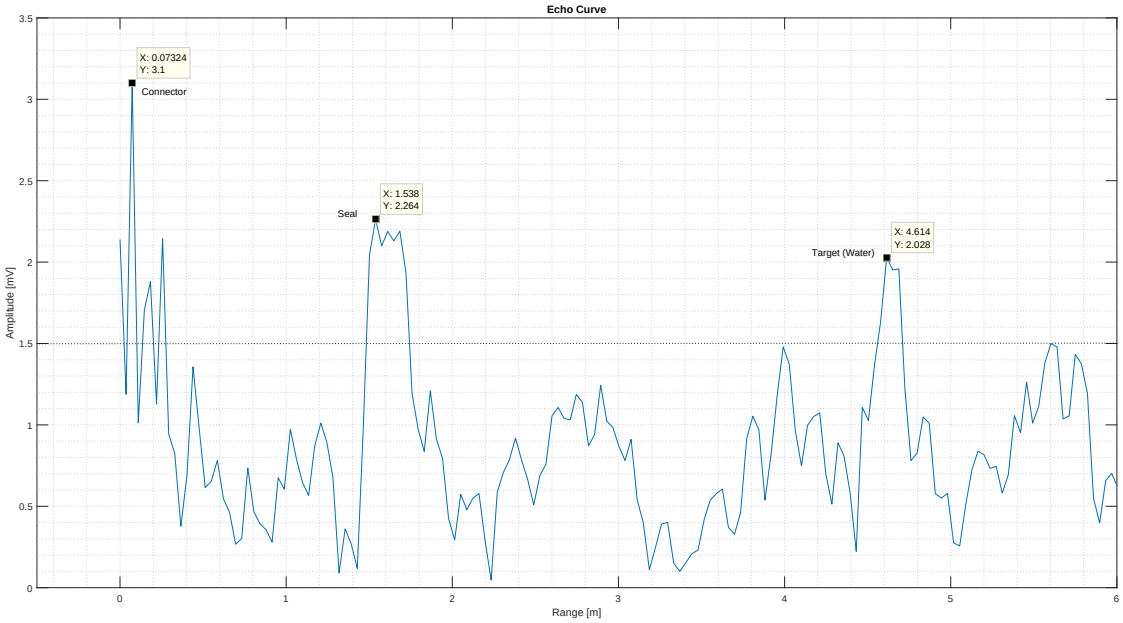

Figure 5.12: Echo curve for 3 m ullage in 3.1 m water pipe

The coaxial cable connecting the transmitter head to the seal is 1 m long, the thickness of the seal is 2 cm and there is an extra mounting pate of 2 mm thickness used. The range shown in X-axis of the curve is considering speed of light $c = 3 \cdot 10^8$ m/s for the signal through all media. However, it is $0.67 \cdot c$ through the coaxial cable. So, the separation between the connector and the seal measured as $1.538 - 0.07324 = 1.465$ m can be converted to $1.465 \cdot 0.67 = 0.981$ m as expected. The ullage measured between the seal and target in the curve is $4.614 - 1.538 = 3.076$ m. When the seal thickness 2 cm and the plate thickness 2 mm were deducted from it, the actual ullage measured becomes 3.052 m. The measurement offset is approximately 52 cm. Considering the noise floor amplitude of 1.5 mV and the target peak of 4.614 mV, the SNR can be calculated as 9.76 dB.

6

Discussion

The chapter contains the more elaborate results obtained which could help in the further study of the technology.

6.1 Comparison Of Sweep Parameters

To compare the performance of different configuration of sweep parameters, we measured a 20 m coaxial cable terminated with ground using different start frequency, stop frequency, step size, etc. The SNR of the target echo, the measured range and the time of measurement are compared in table 6.1. The important reflection from this was the HF sweep alone gives good performance in shorter measurement time.

Fstart (MHz)	**Fstop (MHz)**	**Fstep(MHz)**	**SNR (dB)**	**R (m)**	**Tswp (s)**
1	4096	1	20.11	19.44	9.74
1	4000	1	19.37	19.44	9.29
1	2048	1	20.4	19.44	8.52
1	1024	1	18.32	19.44	8.02
1	300	1	9.64	17.02	7.71
301	4096	1	21.32	19.47	3.18
10	4000	10	14.32	44.68	2.32
35	4096	1	21.54	19.47	3.29
1	4096	1	20.51	19.44	9.33

Table 6.1: Comparison of sweep parameters for a 20 m coaxial cable target

6.2 Impact Of Variable Attenuator In Regulating Transmitted Power

The transmitted power was measured using a spectrum analyser for the entire frequency range from 1 MHz to 4096 MHz in 1 MHz steps and this data was used to configure the attenuator for each step. The power measured for the entire sweep with different configurations of attenuator values is shown in figure 6.1.

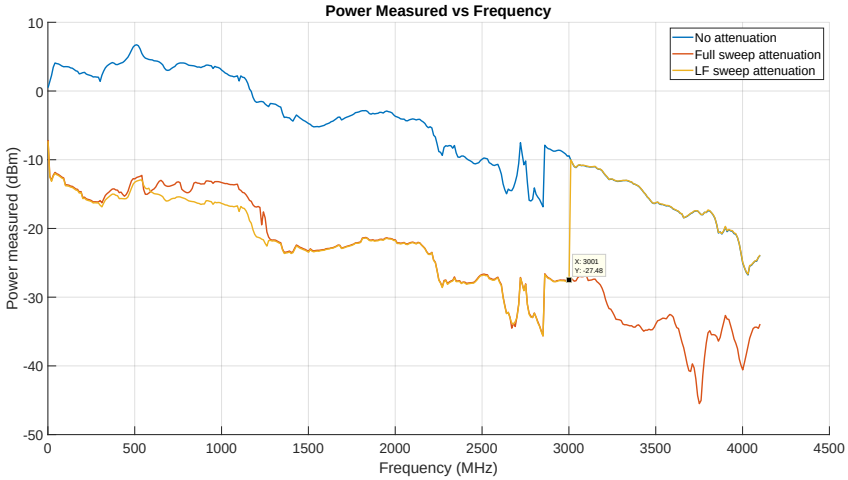

Figure 6.1: Impact of variable attenuator on transmitted power

The echo curve was generated for a coaxial cable terminated by ground at the end with different configurations of attenuator as shown in figure 6.2. SNR without any attenuation is 13.75 dB, whereas SNR with attenuation for complete sweep is 11.40 dB. This proves that applying the attenuator for entire sweep dampens the HF sweep much and affect the SNR. Applying the attenuator for only LF sweep gave an impressive SNR of 20.51 dB.

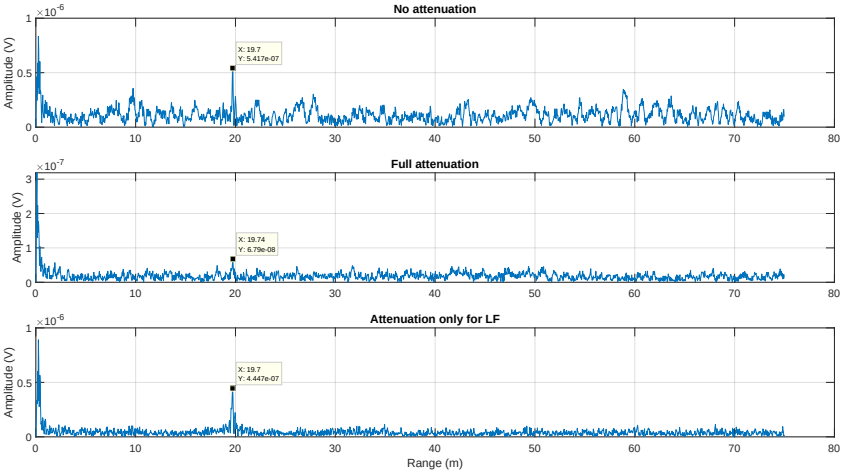

Figure 6.2: Impact of normalizing transmitted power in SNR

6.3 Detailed Analysis Of Power Consumption

The power consumption for different components in our stepped FMCW demonstrator during idle state are shown in table 6.2 below.

Table 6.2: Power consumption in idle state

Part	***Psupply, Idle (mW)***		
	Min	*Avg*	*Max*
MCU STM32U575	19.49	19.98	20.78
TRF37B73EVM Gainblock - 15 dB EVB	170	170	171
ADL5611 Gainblock - 22 dB EVB	483	485	486
AD8342 Downmixer EVB	473	482	484
AD8544 IF Filter + Amplifier PCB	0.48	0.49	0.51
Si5351B LF Synthesizer EVB	329	333	337
ADF4351 HF Synthesizer EVB	16.5	17.1	17.7
AD5160 Digital Potentiometer EVB	0	0.0024	0.16
Demonstrator Total	1491.48	1507.58	1517.16

The power consumption for different components in our stepped FMCW demonstrator during the low frequency sweep are shown in table 6.3 below.

Table 6.3: Power consumption in low frequency sweep

Part	***Psupply, LF sweep (mW)***		
	Min	*Avg*	*Max*
MCU STM32U575	19.82	20.65	22.07
TRF37B73EVM Gainblock - 15 dB EVB	169	170	171
ADL5611 Gainblock - 22 dB EVB	485	487	488
AD8342 Downmixer EVB	481	482	489
AD8544 IF Filter + Amplifier PCB	0.479	0.538	3.24
Si5351B LF Synthesizer EVB	317	350	558
ADF4351 HF Synthesizer EVB	16.5	17.1	17.5
AD5160 Digital Potentiometer EVB	0	0.0071	1.3
Demonstrator Total	1488.80	1527.29	1750.11

The power consumption for different components in our stepped FMCW demonstrator during the high frequency sweep are shown in table 6.4 below.

Table 6.4: Power consumption in high frequency sweep

Part	***Psupply, HF sweep (mW)***		
	Min	*Avg*	*Max*
MCU STM32U575	22.64	23.24	23.83
TRF37B73EVM Gainblock - 15 dB EVB	169	170	171
ADL5611 Gainblock - 22 dB EVB	228	510	912
AD8342 Downmixer EVB	481	484	508
AD8544 IF Filter + Amplifier PCB	0.48	0.52	1.7
Si5351B LF Synthesizer EVB	354	359	376
ADF4351 HF Synthesizer EVB	304	350	426
AD5160 Digital Potentiometer EVB	0	0.01	0.22
Demonstrator Total	1559.12	1896.77	2418.76

The power consumption for different components in our stepped FMCW demonstrator during the post processing state after frequency sweep are shown in table 6.5 below.

Table 6.5: Power consumption during post processing and data transfer

Part	***Psupply, Post processing (mW)***		
	Min	*Avg*	*Max*
MCU STM32U575	20.95	22.34	27.15
TRF37B73EVM Gainblock - 15 dB EVB	169	170	171
ADL5611 Gainblock - 22 dB EVB	488	489	491
AD8342 Downmixer EVB	479	480	481
AD8544 IF Filter + Amplifier PCB	0.51	0.52	0.53
Si5351B LF Synthesizer EVB	328	333	338
ADF4351 HF Synthesizer EVB	16.4	17	17.6
AD5160 Digital Potentiometer EVB	0	0.064	0.40
Demonstrator Total	1501.87	1511.93	1526.69

The power consumption for different components in our stepped FMCW demonstrator when the MCU is in reset are shown in table 6.6 below. The power of the

MCU has reduced much while the others haven't.

Table 6.6: Power consumption when system is in reset

Part	***Psupply,In reset (mW)***		
	Min	*Avg*	*Max*
MCU STM32U575	1.75	2.065	3.95
TRF37B73EVM Gainblock - 15 dB EVB	169	170	171
ADL5611 Gainblock - 22 dB EVB	488	490	491
AD8342 Downmixer EVB	468	478	481
AD8544 IF Filter + Amplifier PCB	0.51	0.52	0.53
Si5351B LF Synthesizer EVB	329	333	338
ADF4351 HF Synthesizer EVB	16.4	17	17.6
AD5160 Digital Potentiometer EVB	0	0.062	0.38
Demonstrator Total	1472.67	1490.65	1502.93

7

Conclusion

The FMCW GWR demonstrator concept was demonstrated successfully in the thesis. Though it offers advantages like avoidance of EMI common to time domain signals, the complex microwave architecture is a major constraint.

One limiting factor is the time it takes to complete one measurement. To get a good resolution, we need to have a very high bandwidth. Optimizing for faster sweep is thus a requirement. High noise floor is another issue faced which can be improved by reducing losses by making a custom PCB for the system. Also, full EM simulations hopefully improve the circuits designed. Further improving sampling and signal processing methods also help in obtaining a cleaner echo curve. Implementing IQ demodulation in hardware could help the sampling by reducing the requirement to one sample per frequency step.

Furthermore, the power consumption for the different microwave components like mixers and gain blocks need to be taken into account in a stepped FMCW system. This can be an issue of exceeding the maximum power consumption in 4-20 mA loop powered safety standard.

Bibliography

[1] P. Mohindru, "Development of liquid level measurement technology: A review," *Flow Measurement and Instrumentation*, vol. 89, p. 102295, 2023. [Online]. Available: https://www.sciencedirect.com/science/article/pii/S0955598622001704

[2] AZoSensors. (2021) Debunking myths surrounding ultrasonic sensor reliability. [Online]. Available: https://www.azosensors.com/article.aspx?ArticleID=2215

[3] A. Krolak, "Know when to use guided wave radar," pp. 1,2, 10 2016. [Online]. Available: https://prod-edam.honeywell.com/content/dam/honeywell-edam/pmt/hps/products/pmc/field-instruments/smartline-level-transmitters/smartline-guided-wave-level-transmitters/pmt-hps-gwr-in-chemical-processing-oct-2016.pdf?download=false

[4] S. Nahar, "Design and implementation of a stepped frequency continuous wave radar system for biomedical applications," *Master's Thesis, University of Tennessee*, 2018.

[5] J. Yang, X. Huang, T. Jin, J. Thompson, and Z. Zhou, "Synthetic aperture radar imaging using stepped frequency waveform," *IEEE Transactions on Geoscience and Remote Sensing*, vol. 50, no. 5, pp. 2026–2036, 2012.

[6] Kusmadi and A. Munir, "Simulation design of compact stepped-frequency continuous-wave through-wall radar," *2015 International Conference on Electrical Engineering and Informatics (ICEEI)*, pp. 332–335, 2015. [Online]. Available: https://api.semanticscholar.org/CorpusID:16783596

[7] A. Depold, S. Erhardt, R. Weigel, and F. Lurz, "A 10 kHz to 6 GHz low-cost vector network analyzer," *Advances in Radio Science*, vol. 19, pp. 17–22, 2021. [Online]. Available: https://ars.copernicus.org/articles/19/17/2021/

[8] K. Parrish, "An overview of FMCW systems in matlab," *Texas Instruments*, 05 2010.

[9] Emerson, "Rosemount 3300 level transmitter product data sheet," 06 2023, [Accessed: April 19, 2024]. [Online]. Available: https://www.emerson.com/documents/automation/product-data-sheet-rosemount-3300-level-transmitter-en-73582.pdf

[10] E. RTR, "Rosemount 5300 level transmitter product data sheet," 12 2023, [Accessed: April 19, 2024]. [Online]. Available: https://www.emerson.com/documents/automation/product-data-sheet-rosemount-5300-level-transmitter-en-73580.pdf

[11] *Digital signal processing for STM32 microcontrollers using CMSIS*, STMicroelectronics Inc., 2 2018, rev. 2.

[12] R. G. Lyons, *Understanding Digital Signal Processing*. Prentice Hall, 2010.

[13] R. Bracewell, *The Fourier Transform and Its Applications*, ser. Circuits and systems. McGraw Hill, 2000. [Online]. Available: https://books.google.se/books?id=ZNQQAQAAIAAJ

[14] "Matlab," https://se.mathworks.com/products/matlab.html, [Accessed: May 05, 2024].

[15] "Ltspice: A spice simulator software, schematic capture and waveform viewer," https://www.analog.com/en/resources/design-tools-and-calculators/ltspice-simulator.html, [Accessed: May 19, 2024].

[16] "KiCad EDA: A cross platform and open source electronics design automation suite," https://www.kicad.org/, [Accessed: May 21, 2024].

[17] "Cogra pro ab," https://www.cogra.se/, [Accessed: May 21, 2024].

[18] *30 MHz to 6 GHz RF/IF Gain Block*, Analog Devices., 9 2013, rev. B.

[19] *31-6000 MHz RF Gain Block*, Texas Instruments., 5 2014, rev. A.

[20] H. Cho, Y. Jung, and S. Lee, "Fmcw radar sensors with improved range precision by reusing the neural network," *Sensors*, vol. 24, no. 1, 2024. [Online]. Available: https://www.mdpi.com/1424-8220/24/1/136

[21] D. Nuessler and J. Jonuscheit, "Terahertz based non-destructive testing (ndt)," *tm - Technisches Messen*, vol. 88, 04 2020.

[22] *Wideband Synthesizer with Integrated VCO*, Analog Devices., 5 2011, rev. A.

[23] *I2C-programmable anny-frequency CMOS clock generator + VCXO*, Skyworks Solutions, Inc., 8 2021, rev. 1.3.

[24] *Manually Generating an Si5351 Register Map for 10-MSOP and 20-QFN Devices*, Skyworks Solutions, Inc., 9 2021, rev. 0.8.

[25] *Active Receive Mixer Low Frequency to 3.8 GHz*, Analog Devices., 9 2006, rev. C.

[26] ARM Limited, "CMSIS-DSP: ARM digital signal processing library," https://arm-software.github.io/CMSIS_5/DSP/html/index.html, 2024, accessed: 2024-08-07.

A

Appendix 1

A.1 Python Script For Power Measurement Via RS FSP-40 Spectrum Analyser

```
import time
import pandas as pd
from RsInstrument.RsInstrument import RsInstrument

resource_string = 'GPIB0::15::0::INSTR'  # GPIB Connection
instr = RsInstrument(resource_string, True, False)

idn = instr.query_str('*IDN?')
print(f"\n'{idn}'")
print(f'RsInstrument driver version: {instr.driver_version}')
print(f'Visa manufacturer: {instr.visa_manufacturer}')
print(f'Instrument full name: {instr.full_instrument_model_name}')
print(f'Instrument installed options: {",".join(instr.instrument_options)}')

instr.write('*RST;*CLS')
instr.write('FREQ:SPAN 20kHz')
instr.write('BAND 300Hz')
instr.write('DISP:TRAC:Y:RLEV 20dBm')
# instr.write('INIT:CONT OFF')

freq = list(range(1, 4102, 10))
peak = [0] * len(freq)
freq_mes = [0] * len(freq)
freq_off= [0] * len(freq)

instr.write('FREQ:CENT 1MHz')
print('Print here ----------------')

for n in range(len(freq)):

    instr.write('TRIG:SOUR EXT')
    instr.write('INIT:CONT OFF')  # Disable continuous sweep

    freq_str = 'FREQ:CENT {}MHz'.format(freq[n])
    instr.write(freq_str)
    #time.sleep(0.3)

    peak[n] = instr.query_str('CALC:MARK:MAX;Y?')
    freq_mes[n] = instr.query_str('CALC:MARK:MAX;X?')
    freq_mes[n]=float( freq_mes[n])/1000000
    freq_off[n]=(freq[n]-freq_mes[n])*1000
    instr.write('INIT:IMM; *WAI')  # Trigger an immediate measurement and wait for completion


    print('Center Frequency = {}MHz and peak = {}dBm, Frequency offset = {}kHz'.format(freq_mes[n], peak[n],freq_off[n]))
    freq1 = pd.DataFrame(freq, columns=['freq'])
    peak1 = pd.DataFrame(peak, columns=['peak'])
    freq_off1 = pd.DataFrame(freq_off, columns=['freq_off'])

    T = pd.concat([freq1, peak1,freq_off1], axis=1)
    T.to_csv('testfile.txt', sep=' ', index=False)




# Close the session
instr.close()
```

Figure A.1: Python script for controlling and measuring power for 1MHz to 4101 MHz sweep

B

Appendix 2

B.1 Evaluation Setup

The evaluation boards for the system components were procured and the system was created using coaxial cable interconnections in RF and jumper wires for the digital and IF signals. The evaluation setup for the radar used is shown in figure B.1.

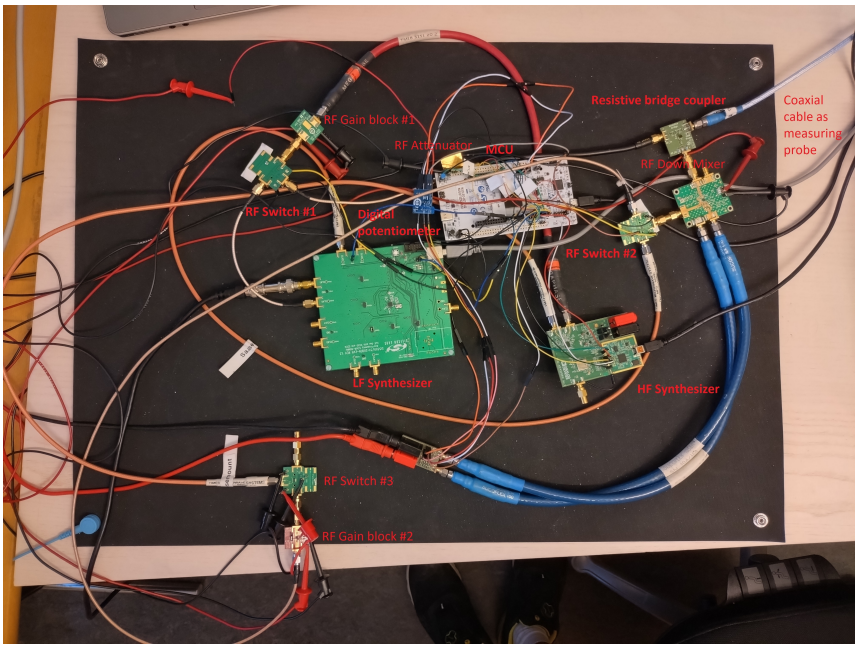

Figure B.1: Evaluation setup for the stepped FMCW radar

The different hardware components used for the demonstrator are shown in figure B.2.

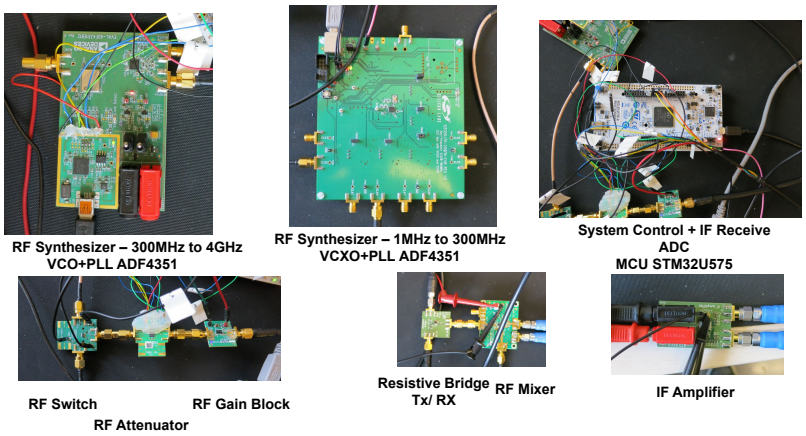

Figure B.2: Hardware components of stepped FMCW demonstrator

C

Appendix 3

C.1 Tank Measurement Setup

The radar was tested with a 4 inch diameter 3.1 m long water pipe whose level was altered via computer software. The pipe measured is shown in figure C.1.

Figure C.1: Water pipes used for measurement

The measurement setup used is shown in figure C.2.

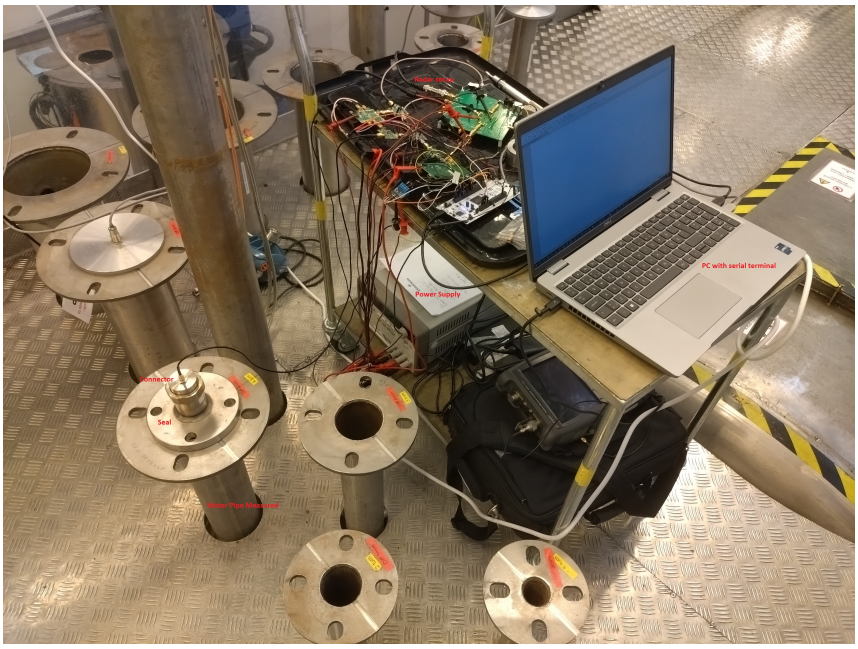

Figure C.2: Connection diagram for the test setup

C.2 Tank Measurements

The radar designed was tested in 3.1 m water pipes with various level configurations other than 3m ullage. Figure C.3 shows the echo curve obtained for a water level of 100 cm and an ullage of 2 m. The measurement was done with a rigid probe and a standard seal. The SNR was measured to be 1.43 dB.

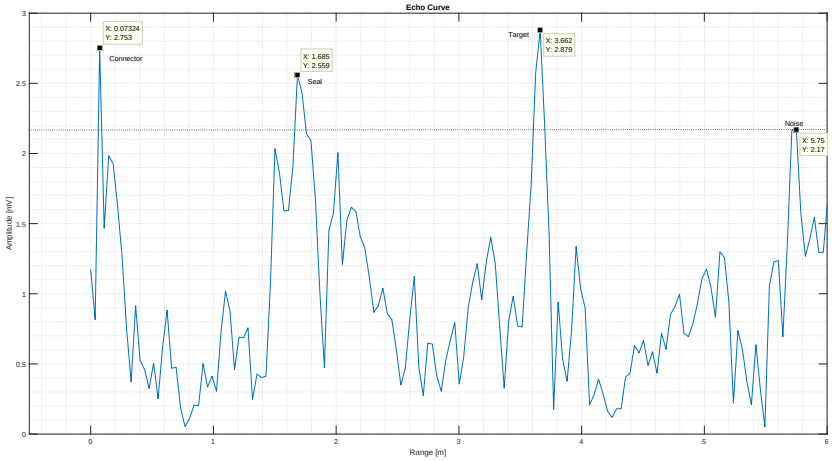

Figure C.3: Echo curve for 2 m ullage in 3.1 m water pipe

Figure C.4 shows the echo curve obtained for a water level of 100 cm and an ullage

of 2 m. The measurement was done with a rigid probe and a standard seal. The SNR was measured to be 3.65 dB.

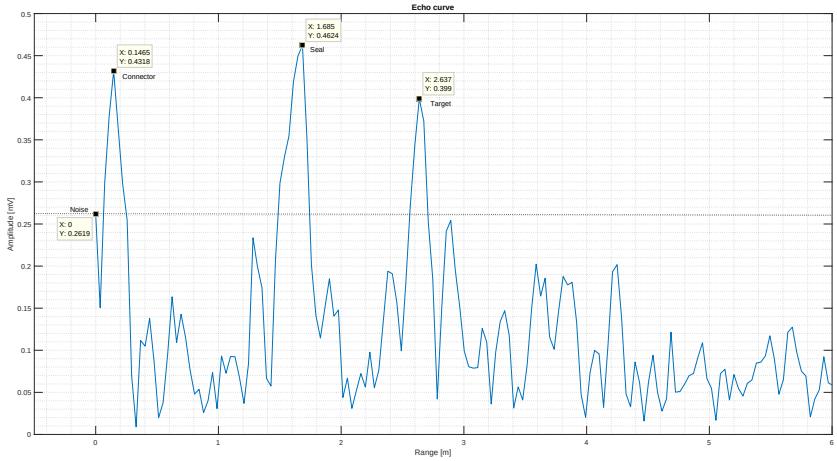

Figure C.4: Echo curve for 1 m ullage in 3.1 m water pipe